Response to Reviewers' Comments

We thank the reviewers for his/her careful reading of our manuscript and insightful comments and suggestions on greatly improving the quality of this manuscript. We address the referees' specific comments point-by-point below. The changes made to the revised manuscript were marked in orange.

Referee #1

This paper investigates the effect of NH3 concentration on NH3 partitioning to the particle phase and the influence of other factors, such as the concentration of a group of PM2.5 inorganic aerosol (sulfate, nitrate, ammonium; SNA) and ambient conditions in a region with very high NH3 plus NH4+ concentrations (ie, ammonia emissions). The title implies that the paper will investigate the overall influence of ammonia on PM2.5 haze, but this is never really done; eg, what fraction of the PM2.5 mass is ammonium, how does high ammonium affect the particle concentrations of Cl-, NO3-, what faction of the PM2.5 mass are these species?

Thanks for the comment. We have added a new section below in the Results and Discussion part to address the concern raised by the reviewer. The high ammonium concentration facilitates water uptake and enhance the aerosol water content. The elevated aerosol water serves as aqueous medium for uptake of reactive gases and promotes the gas-particle partitioning of semi-volatile species (e.g., HCl, HNO3, NH3 and certain organics), thus accelerating the mass growth of aerosol particles.

3.1 Overview of 1 year continuous measurements at Chongming

Figure 1 shows the time-series of hourly water-soluble $PM_{2.5}$ species during the study period. The mean concentration of NO_3^-, SO_4^{2-}, NH_4^+ and Cl^- over the entire study period was 8.4 μg m^{-3}, 6.3 μg m^{-3}, 6.3 μg m^{-3} and 1.2 μg m^{-3}. The haze period was defined as hourly averaged $PM_{2.5}$ mass loadings higher than 75 μg m^{-3} and the rest was non-haze period. Table 1 gives the statistical summary of major aerosols during the haze and non-haze period. Clearly, the mass concentration of major $PM_{2.5}$ species (NO_3^-, SO_4^{2-}, NH_4^+ and Cl^-) increased during the haze period compared to those during the non-haze period. However, the concentration of NH_3 showed no significant change during these two periods. The mean mass concentration of SNA (sulfate, nitrate, and ammonium) was 49.0 μg m^{-3}, contributing to about 50.0 % of total $PM_{2.5}$ mass.

Table 1. Statistical summary on mass concentrations of $PM_{2.5}$ species and NH_3.

Unit: μg m^{-3}	$PM_{2.5}$	SO_4^{2-}	NO_3^-	Cl^-	NH_4^+	NH_3
non-haze	28.5 ± 16.9	5.6 ± 3.6	6.9 ± 6.6	1.1 ± 0.9	5.6 ± 3.3	32.2 ± 11.6
haze	98.3 ± 37.2	13.3 ± 7.7	23.1 ± 14.5	2.2 ± 1.9	13.2 ± 6.6	32.3 ± 13.5

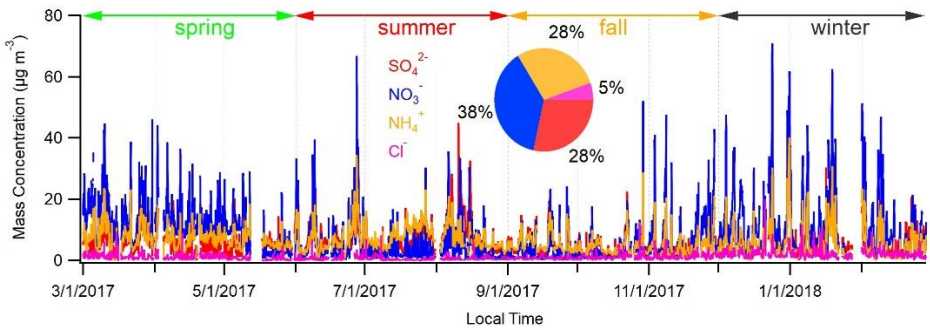

Figure 1: Time series of $PM_{2.5}$ species during the study period.

The analysis includes a thermodynamic model, with the focus of the paper solely on predictions of NH3/NH4+. Since the thermodynamic predictions depend on sulfate and nitrate, along with ammonium, (and possibly chloride) these species should be included in the data presentation and discussion, but are largely ignored. For example, one should also present the partitioning (S curves) of nitrate, and possibly even chloride since it's concentrations are also fairly high (Fig 2) since these species are critical to the thermodynamic predictions and are highly hygroscopic and affect the aerosol liquid water. Overall the data is interesting, but the data analysis should be much more comprehensive and in depth.

Thanks for pointing out this. We agree with the reviewer that the partitioning (S curves) of nitrate, and chloride are critical to the thermodynamic predictions. However, it should be noted that the partitioning ratios (i.e., $\varepsilon(NO_3^-), \varepsilon(Cl^-)$) should be close to 50% in order to be useful for assessing the ISORROPIA II predictions(Guo et al., 2017). But this is not the case in this study especially for the winter haze period when gas phase HCl and gas phase HNO_3 only accounting for less than 4% of the total chloride and total nitrate. For example, the hourly HCl mass concentration was below the detection limit of the instrument during more than 70% of the winter season. And the detectable HNO_3 mass concentration in winter was around 0.4 μg m^{-3} compared to about 11.8 μg m^{-3} of nitrate in the particulate phase. Given that this paper focused on the haze pollution that mostly occurred in winter, we limited our discussion on the partitioning ratios of $\varepsilon(NH_4^+)$, which was close to 50% during the winter season as shown in figure 6.

In response, we plotted the following figure that shows the predicted vs measured HNO_3 and HCl, respectively. This figure has been added to the supplementary materials in the revision.

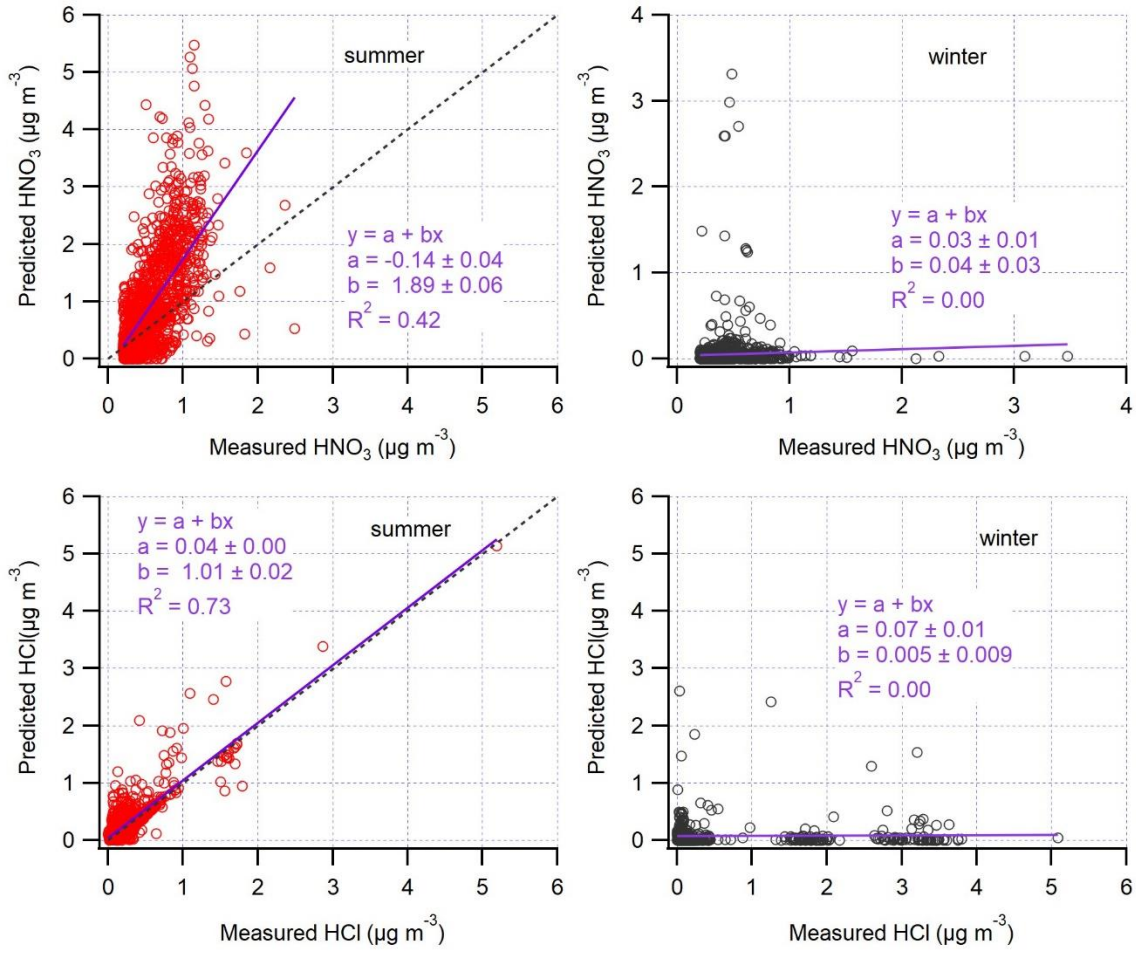

Figure R1: Comparison of predicted and measured HNO_3 and HCl in summer and in winter. Orthogonal distance regression (ODR) fits with ±1σ are shown.

Specific Comments

Was there even any mention of the sulfate concentration in this study?

Thanks for the comment. Sulfate concentration can be found in the new section 3.1. The mean concentration of SO_4^{2-} over the entire study period was 6.3 μg m^{-3}. And the newly added table 1 gives the mean concentration of SO_4^{2-} during the haze (13.3 ± 7.7 μg m^{-3}) and non-haze (5.6 ± 3.6 μg m^{-3}) period.

The ACR is widely used in this paper and defined in the Abstract as the ammonia gas-particle conversion ratio, but that is ambiguous, explicitly define it in the Abstract. I strongly suggest the authors use a more common term, epsilon(NH4+), why make up new terminology?

Thanks for pointing out this. We have changed ammonia gas-particle conversion ratio into $\varepsilon(NH_4^+)$ throughout the manuscript.

How was the TEOM sample air dried? What was the temperature if dried? How would it affect mass concentrations of semivolatile species, such as NH4NO3?

Thanks for the comment. TEOM sample air was dried through the filter dynamics measurement systems (FDMS). FDMS was equipped in TEOM 1405-F to account for both the volatile and non-volatile species of fine particles. According to the guidelines released by Thermo Scientific, *this is done by measuring the volatile portion of the sample independently from the total incoming sample, and using this fraction in calculating the PM mass concentration. FDMS dryer contains specially-designed Nafion tubing inlet on the main flow to minimize potential for particle loss. The dryer lowers the main flow relative humidity, and allows for mass transducer operation at 5 ℃ above the peak air monitoring station temperature. Purge Filter Conditioner contains a heat exchanger that maintains the temperature of the main air flow and particle filter at 4 ℃. An integrated humidity sensor that follows the SES dryer measures the main flow line humidity to determine the drying efficiency*.

Although PM2.5 mass and various gas phase species measurement methods are discussed, the data are really never considered in any important way, so why discuss the measurement method?

Thanks for pointing out this. The gas phase species measurement methods were deleted in the revision. Section 2.2 has been changed as below:

"……Meanwhile, ~~$PM_{2.5}$ and gaseous pollutants (SO_2, NO_2, O_3, and CO) were monitored by co-located instruments. M~~mass loadings of $PM_{2.5}$ was determined by a Tapered Element Oscillating Microbalance coupled with Filter Dynamic Measurement System (TEOM 1405-F). ~~SO_2 mass concentrations were analyzed by Pulsed Fluorescence SO_2 Analyzer (Thermo Fisher Scientific, Model 43i). NO_2 mass concentrations were analyzed by Chemiluminescence NO-NO_2-NO_x Analyzer (Thermo Fisher Scientific, Model 42i). O_3 mass concentrations were analyzed by UV Photometric Ozone Analyzer (Thermo Fisher Scientific, Model 49i). CO mass concentrations were analyzed by Gas Filter Correlation CO Analyzer (Thermo Fisher Scientific, Model 48i).~~ The QA/QC of these instruments were managed by professional staff in Shanghai Environmental Monitoring Center (SEMC) according to the Technical Guideline of Automatic Stations of Ambient Air Quality in Shanghai (HJ/T193-2005)."

Figure 2. No explanation is given on why both gas/particle data are compared for ammonia but not for chloride or nitric acid. Also it would be insightful to plot ACR predicted vs measured, and plot and discuss the gas phase components of Cl- and NO3-, as was done for NH4+/HNO3. These comparisons, are also important to assess the model.

Thanks for pointing out this. As responded above, the measured concentration of HNO_3 and HCl in the gas phase in winter was close to the detection limit of the instrument and much lower than the nitrate and chloride in the particle phase, respectively. Given that this paper focused on the haze pollution that mostly occurred in winter, we only show the gas/particle data comparison for ammonia but not for chloride or nitric acid in the original manuscript. In response, we plotted the following

figure that shows the predicted vs measured HNO_3 and HCl, respectively. This figure has been added to the supplementary materials in the revision.

We agree with the reviewer that the partitioning (S curves) of nitrate, and chloride are critical to the thermodynamic predictions. And it should be noted that the partitioning ratios (i.e., $\varepsilon(NO_3^-), \varepsilon(Cl^-)$) should be close to 50% in order to be useful for assessing the ISORROPIA II predictions. However, this is not the case in this study especially for the winter haze period when gas phase HCl and gas phase HNO_3 only accounting for less than 4% of the total chloride and total nitrate. For example, the hourly HCl mass concentration was below the detection limit of the instrument more than 70% of the winter season. And the detectable HNO_3 mass concentration in winter was around 0.4 μg m^{-3} compared to about 11.8 μg m^{-3} of nitrate in the particle phase. Given that this paper focused on the haze pollution that mostly occurred in winter, we limited our discussion on the partitioning ratios of $\varepsilon(NH_4^+)$, which was close to 50% during the winter season as shown in figure 6 in the manuscript.

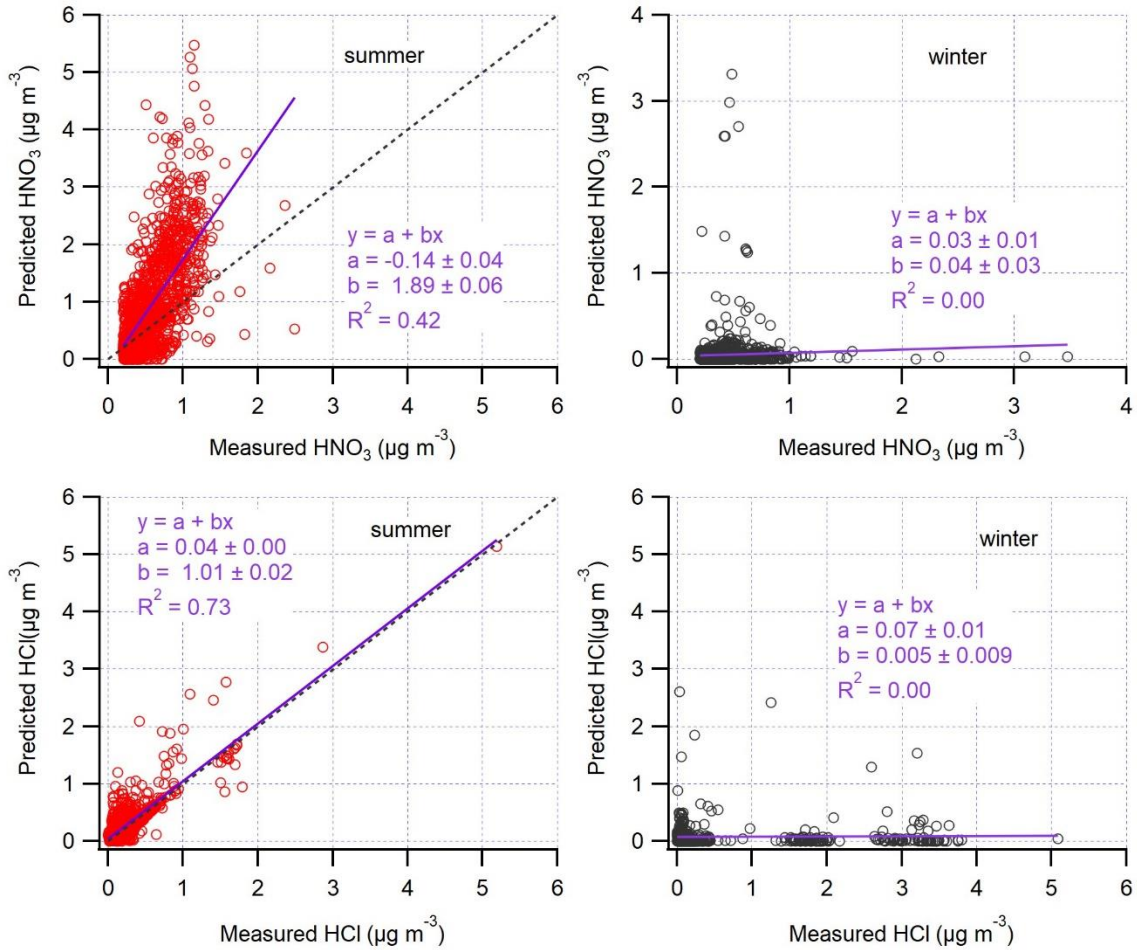

Figure R1: Comparison of predicted and measured HNO_3 and HCl in summer and in winter. Orthogonal distance regression (ODR) fits with ±1σ are shown.

Since concentrations of the important other inorganic ions other than just NH4+ are not presented, the analysis in this paper is largely superficial. For example, roughly what is the form of the ammonium in the particle, is it ammonium nitrate, ammonium sulfate, ammonium chloride? Why not give a pie chart of the inorganic species concentrations, as noted above regarding sulfate, no data on these other important species are given.

Thanks for the comment. If we assume ammonium was preferably neutralized by sulfate than nitrate when NH_3 was in excess. Roughly 47% of ammonium was expected to be in the form of ammonium sulfate during the winter haze period. And ammonium nitrate dominates the remaining part of

ammonium. We have added a new section below in the Results and Discussion that shows inorganic species concentrations.

3.1 Overview of 1 year continuous measurements on Chongming

Figure 1 shows the time-series of hourly water-soluble $PM_{2.5}$ species during the study period. The mean concentration of NO_3^-, SO_4^{2-}, NH_4^+ and Cl^- over the entire study period was 8.4 μg m^{-3}, 6.3 μg m^{-3}, 6.3 μg m^{-3} and 1.2 μg m^{-3}. The haze period was defined as hourly averaged $PM_{2.5}$ mass loadings higher than 75 μg m^{-3} and the rest was non-haze period. Table 1 gives the statistical summary of major aerosols during the haze and non-haze period. Clearly, the mass concentration of major $PM_{2.5}$ species (NO_3^-, SO_4^{2-}, NH_4^+ and Cl^-) increased during the haze period compared to those during the non-haze period. However, the concentration of NH_3 showed no significant change during these two periods. The mean mass concentration of SNA (sulfate, nitrate, and ammonium) was 49.0 μg m^{-3}, contributing to 50.0 % of total $PM_{2.5}$ mass.

Table 1. Statistical summary on mass concentrations of $PM_{2.5}$ species and NH_3.

Unit: μg m^{-3}	$PM_{2.5}$	SO_4^{2-}	NO_3^-	Cl^-	NH_4^+	NH_3
non-haze	28.5 ± 16.9	5.6 ± 3.6	6.9 ± 6.6	1.1 ± 0.9	5.6 ± 3.3	32.2 ± 11.6
haze	98.3 ± 37.2	13.3 ± 7.7	23.1 ± 14.5	2.2 ± 1.9	13.2 ± 6.6	32.3 ± 13.5

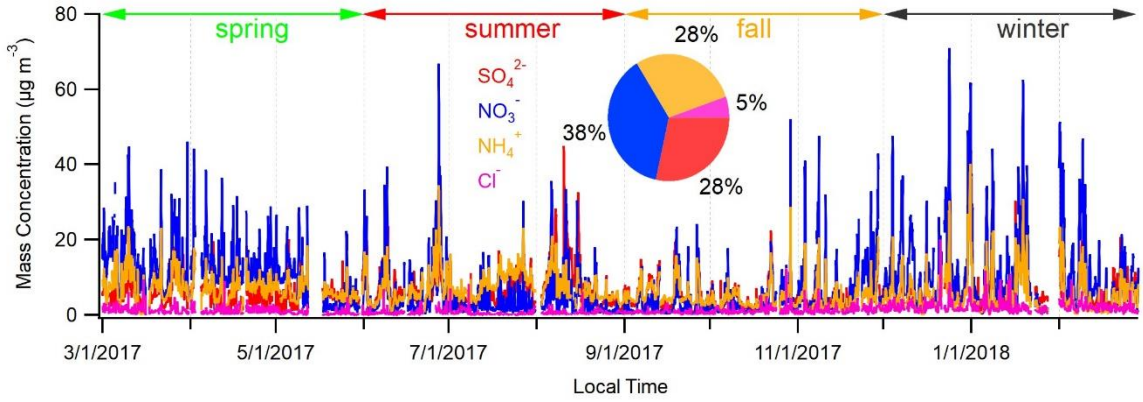

Figure 1: Time series of $PM_{2.5}$ species during the study period.

In Fig 4 the number of data points are not considered in the statistical results. Instead of plotting the error bar as the standard deviation plot it as the standard error, or better yet make bar-whisker plots instead. Does average = mean (mean is the more explicit term)? There is clearly a temp trend in this Fig, which should be explicitly discussed, ie, this plot simply shows that lower T more partitioning to the aerosol higher leading to high SNA and lower NH3 (if SNA is dominated by NA and not S).

Thanks for the comment. We have added the number of data points in Figure 4. The bar-whisker plot has been inserted into the new figure 4 as below in the revision. Yes, here "average" means "mean" and the term "average" is replaced by "mean" throughout the manuscript. We did a statistical analysis of SNA concentration versus temperature (T). T has been divided into <0, 0~10, 10~20, 20~30, and >30 ◦C, the resulting mean SNA concentration was 21.1, 24.8, 21.3, 17.9 and 20.0 μg m^{-3}, respectively. Hence, there were no significant differences of SNA under different bins of temperature. We agree with the reviewer that temperature plays an important role in the SNA formation. However, as we pointed out throughout the MS, other factors including pH, aerosol water content and activity coefficients ratio of $\frac{\gamma_{H^+}}{\gamma_{NH_4^+}}$ also affect the SNA formation.

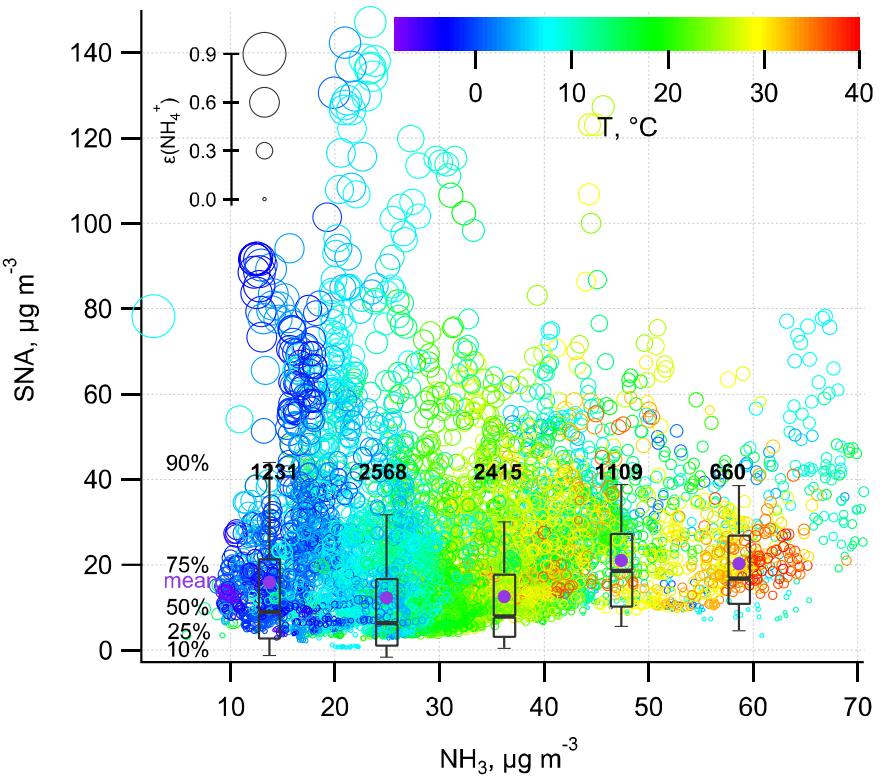

Line 152. ISORROPIA is used for the predictions (ie, LWC, pH) and activity coefficients for the S curve are taken from E-AM. Is it reasonable to mix these two models? How do these activity coefficients compare to that predicted by ISORROPIA.

Thanks for the comment. We have re-calculated and re-plotted the S curve using activity coefficients taken from ISORROPIA II with the help of our co-author Dr. Hongyu Guo. For example, figure 6 has been replotted with $\frac{\gamma_{H^+}}{\gamma_{NH_4^+}}$ predicted by ISORROPIA II in the revision. Note the S curve only shifted to the right after the input of $\frac{\gamma_{H^+}}{\gamma_{NH_4^+}}$ changed from 2.4 ± 2.0 to 4.0 ± 2.6.

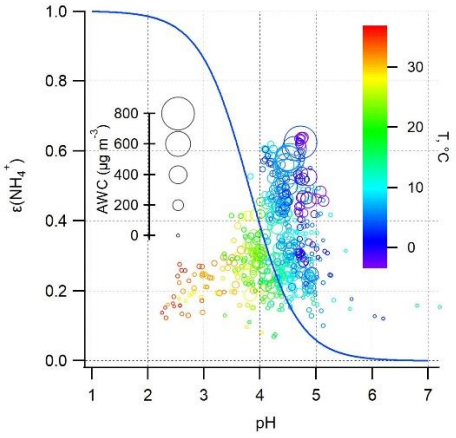

Figure 6: $\varepsilon(NH_4^+)$ as a function of pH during the haze period. The sizes of the void circles are scaled to AWC and colored by T. The blue curve was calculated based on the average T (10 ℃), AWC (100 μg m^{-3}), and activity coefficients ratio of $\frac{\gamma_{H^+}}{\gamma_{NH_4^+}}$ respectively. The average $\frac{\gamma_{H^+}}{\gamma_{NH_4^+}}$ for the haze period is 4.0 ± 2.6 (±1σ).

Line 135. The statement that NH3 concentration can be interpreted as the strength of the NH3 emissions is true only if only a small fraction of the total NH3 can be in the particle phase, which ACR shows is not true.

Thanks for the comment. It should be noted that NH_3 means gas phase ammonia in the manuscript.

The table in the supplemental data is cut off and not all is legible.

Thanks for pointing out this. We have re-sized the columns of Table S1 in the revised version.

Fig 6. The comparison between the S curve and the data is claimed to be good (relatively well constrained), but is it? Compare this result to other published identical plots and discuss why there appears to be more (or maybe less) discrepancy in this study. S curves of nitrate and possibly chloride should be included since the data exits and they can also be used to assess the thermodynamic model.

Thanks for the suggestion. The S curve in Fig. 6 represents the relationship between $\varepsilon(NH_4^+)$ and pH based on the mean condition of the winter haze period, i.e. T of 10 ℃ and AWC of 100 μg m-3. As the observational data points in Fig. 6 covered data during the whole study period, it is reasonable that some data points didn't distribute along the curve. Using the same methodology as figure 4 in Nah et al., 2018, we picked a small range of AWC (80 to 120 μg m^{-3}) and T (8 to 12 ◦C) to be close to the average AWC (100 μg m^{-3}) and T (10 ◦C) during the haze period. We calculated the S curve of $\varepsilon(NH_4^+)$ with the average AWC and T and plot the selected dataset in Figure R2 as below. Clearly, for the data points selected, there is roughly the same amount of spread compared to Nah et al., 2018.

We agree with the reviewer that the partitioning (S curves) of nitrate, and chloride are critical to the thermodynamic predictions. However, note that the partitioning ratios (i.e., $\varepsilon(NO_3^-), \varepsilon(Cl^-)$) should be close to 50% in order to be useful for assessing the ISORROPIA II predictions(Guo et al., 2017). But this is not the case in this study especially for the winter haze period when gas phase HCl and gas phase HNO_3 only accounting for less than 4% of the total chloride and total nitrate. For example, the hourly HCl mass concentration was below the detection limit of the instrument more than 70% of the winter season. And the detectable HNO_3 mass concentration in winter was around 0.4 μg m^{-3} compared to about 11.8 μg m^{-3} of nitrate in the particle phase. Given that this paper focused on the haze pollution that mostly occurred in winter, we limited our discussion on the partitioning ratios of $\varepsilon(NH_4^+)$, which was close to 50% during the winter season as shown in figure 6.

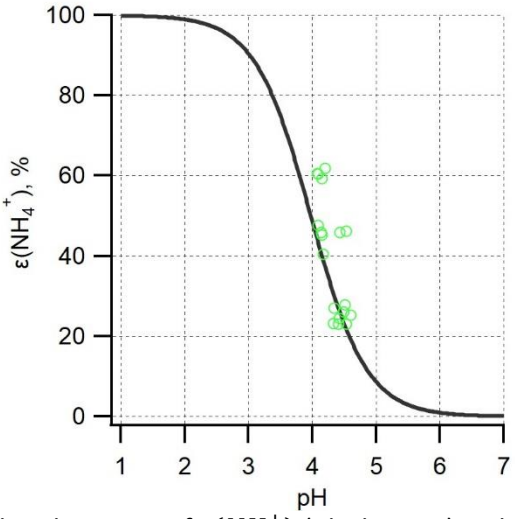

Figure R2: Analytically calculated S curves of $\varepsilon(NH_4^+)$ (Black curve) and measured $\varepsilon(NH_4^+)$ (void green circles) as a function of pH. A small range of AWC (80 to 120 μg m^{-3}) and T (8 to 12 ◦C) to be close to the average AWC (100 μg m^{-3}) and T (10 ◦C) was selected during the haze period. The S curve was calculated based on the average T (10 ℃), AWC (100 μg m^{-3}), and activity coefficients ratio of $\frac{\gamma_{H^+}}{\gamma_{NH_4^+}}$

(6.0) respectively. Note the average $\frac{\gamma_{H^+}}{\gamma_{NH_4^+}}$ for the selected ambient data we used to calculate the S curve is 6.0 not 4.0.

Lines 162-165. This explanation does not make sense. The model predicts the equilibrium state, which should exist at all time since the time scales to reach it are about 30 minutes. How will long range transport effect that. The authors need to investigate the thermodynamic model predictions better and come up with a better discussion.

Thanks for pointing out this. We agree with the reviewer that long range transport would not affect the equilibrium. After re-calculating the possible effect from organic mass as shown in Figure R3 below, we have deleted these texts.

Line 169. If the authors are going to accept the Silvern et al theory of a film impeding uptake of NH3, then they cannot accept the results of their thermodynamic analysis. Or they must assume that it affects only a fraction of the aerosol. This needs more explanation.

Thanks for the comment. Silvern et al., 2017 suggested that inorganics particles are coated by organic film, impeding the uptake of ammonia. The presence of organics was expected to slow down the achievements of inorganic thermodynamic equilibrium. We agree with the reviewer that the organic coating affects only a fraction of the inorganic aerosol and the thermodynamic equilibrium were assumed to achieve within one hour even organic films present.

Overall, the explanations for the discrepancy is largely just throwing out ideas and not assessing quantitatively the effect. For example, if the AWC is 35% higher how does that affect the S curve and data in Fig. 6. How will a different Henry's law affect the S curve in Fig 6 (ie which way is it shifted, to better or worse agreement with the data)?

Thanks for the comment. The discrepancy has been quantitatively analyzed as below in the revision. Since the mass concentration of organic aerosol was not available in this study, We did a sensitivity analysis via increasing the AWC by 10, 20 to 90 μg m^{-3} as shown in Figure R3. The pH was not re-calculated using the new AWC because the co-existed organic aerosol altered pH in a complex way (Battaglia Jr et al., 2019;Wang et al., 2018;Pye et al., 2020). For example, some organic acids increase aerosol acidity thus decrease pH, whereas organic basics (e.g., amines) raise aerosol pH. We found that the best agreement between the predicted and measured $\varepsilon(NH_4^+)$ was achieved when we increase the AWC by roughly 90 μg m^{-3}, suggesting a nearly 48% of AWC contributed by the organics. This result falls in the range from a recent report in North China that organics contribute to 30 % ± 22% of AWC (Jin et al., 2020), and slightly higher than those southeastern United States sites that organic aerosol-related water accounting for about 29 to 39% of total water (Guo et al., 2015) and those in the eastern Mediterranean that about 27.5% of total aerosol water resulted from organics (Bougiatioti et al., 2016).

A higher Henry's law constant shift the S curve to the right and a lower Henry's law constant shift the S curve to the left.

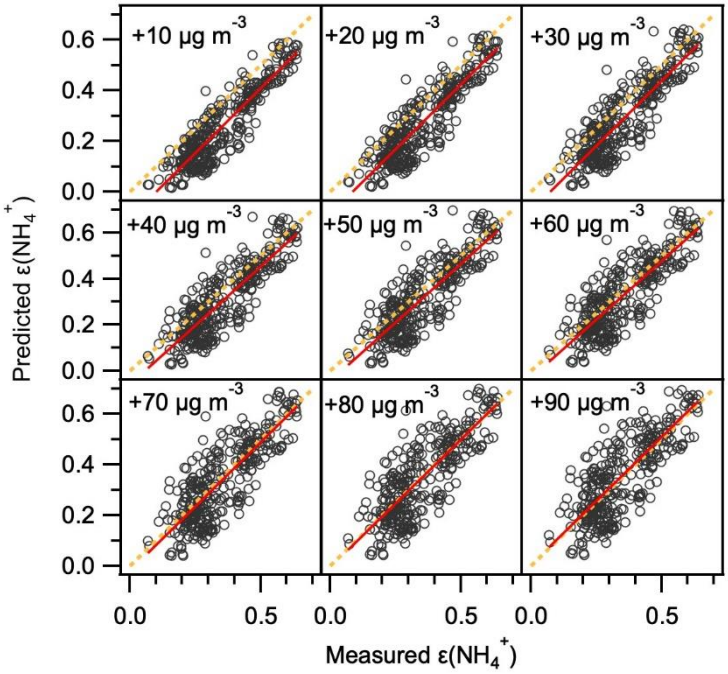

Figure R3: Comparison of predicted and measured $\varepsilon(NH_4^+)$. Note the predicted $\varepsilon(NH_4^+)$ was analytically calculated using the equation 2 with input (i.e., pH, AWC, $\frac{\gamma_{H^+}}{\gamma_{NH_4^+}}$) taken from ISORROPIA II prediction and the AWC has been increased by 10, 20 to 90 µg m^{-3} while other inputs fixed. Orthogonal distance regression (ODR) fits line (red) and y=x line (dashed orange) was shown for the clarity of the figure.

Line 183 to 185. How does the affect of ALW on secondary aerosol formation (ie, I assume here from the references the authors are referring to SOA formation) affect the ACR?

Thanks for the comment. The authors want to mention the AWC has also been known to enhance SOA formation. However, the enhanced SOA formation resulting from AWC may not affect the ACR or possible affecting the ACR in the same way as those semi-volatile inorganics.

The text has been revised as "AWC has also been known to promote secondary organic aerosol formation by providing aqueous medium for uptake of reactive gases, gas to particle partitioning, and the subsequent chemical processing (McNeill, 2015;McNeill et al., 2012;Tan et al., 2009;Xu et al., 2017)."

Fig 9, ACR vertical axis is not colored the same way as the line on the plot (black and not yellow), whereas for the other plotted components there is consistency.

Thanks for pointing out this. The ACR vertical axis has been changed to yellow color as below in the revision.

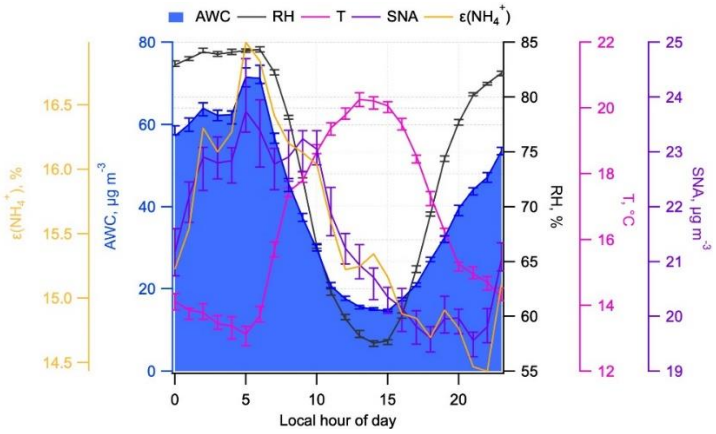

Section 3.3 Please explain the logic why similar diurnal trends in SNA, ACR and AWC at night supports the self amplifying feedback loop in SNA formation. Also how specifically does daytime photochemistry lead to a discrepancy if it is always assumed that the aerosol is in equilibrium?

Thanks for the comment. We understand that if the self-amplifying feedback mechanism dominate the SNA formation, then the diurnal trends of SNA, ACR and AWC would track each other. In Figure 9, we saw similar diurnal trends in SNA, ACR and AWC at night. So the self-amplifying feedback mechanism can be verified during the nighttime. But the daytime SNA concentration did not show similar variation as ACR and AWC, so we expect other mechanism also in play. Since the trend deviation of SNA concentration happened during the mid-afternoon when strong photochemical activity occurs. Therefore, we assume both the self-amplifying feedback mechanism and photochemical production was in play during the daytime while self-amplifying feedback mechanism dominate the SNA formation at night.

SNA includes sulfate. How does sulfate play a role in this feedback mechanism?

Thanks for the comment. SNA includes sulfate, and after the initial formation of SNA triggered by the gas-particle conversion of NH_3, the sulfate, together with nitrate and ammonium, promotes water uptake and resulted in the increase of aerosol water content. Then the increase of aerosol water content further raise the $\varepsilon(NH_4^+)$ and more SNA formed. So the role of sulfate in the feedback mechanism is to facilitate water uptake.

The idea of feedback (or sometimes called co-condensation) leading to more uptake of NH3 by the added liquid water is not a new concept. It happens for any semi-volatile species that when partitioned to the particle phase significantly increases the water uptake. Thus, since sulfate is not semi-volatile and highly hygroscopic the species involved must generally have significantly higher concentrations then sulfate. Essentially here the effect is due to ammonium nitrate uptake, the same process discussed in Guo et al. (2017), yet here the focus is just on NH3/NH4+, the role of nitrate and possibly chloride in this process should also be included in the analysis. Note, that the molecular weight of NO3is > NH4+ (thus most have focused on NO3since one is generally concerned with effects on PM mass. Since the authors seem to think this is an important result from this work, they should discuss this process in much more detail and cite other papers that have also investigated the process. See, for example Topping et al (2013).

Guo, H., J. Liu, K. D. Froyd, J. Roberts, P. R. Veres, P. L. Hayes, J. L. Jimenez, A. Nenes, and R. J. Weber (2017), Fine particle pH and gas-particle phase partitioning of inorganics in Pasadena, California, during the 2010 CalNex campaign, Atm. Chem. Phys., 17, 5703-5719.

Topping, D., P. Connolly, and G. McFiggans (2013), Cloud droplet number enhanced by co-condensation of organic vapours, Nature Geoscience, 6, 443-446.

Thanks for the comment. We agree with the points raised by this reviewer that "since sulfate is not semi-volatile and highly hygroscopic the species involved must generally have significantly higher concentrations then sulfate". Nitrate is more hygroscopic than sulfate and the mass concentration of

nitrate was indeed significantly higher than sulfate in this study (Table 1). And the work by Topping (Topping et al., 2013) has been cited in the revision below.

Given that AWC is a function of RH and SNA, a conceptual model of how AWC control ACR can be illustrated by a self-amplifying feedback loop (Figure 8). Formation of SNA is initiated by gas-particle conversion of NH_3. Under certain meteorological conditions such as high RH and shallow planetary boundary layer, SNA is subject to uptake moisture and result in the increases of AWC. The enhanced aerosol water dilutes the vapor pressure of semi-volatile species (i.e., nitrate, ammonium and chloride) above the particle and driving semi-volatile species continue to condense (Topping et al., 2013). Based on the discussions above, the increase of AWC would further raise ACR, leading to more efficient transformation of NH_3 as SNA.

Referee #3

Secondary inorganic aerosol are major fractions of PM2.5 in China, especially during the hazy episode. Xu et al. investigate the role of ammonia gas-particle conversion ratio on secondary inorganic aerosol formation mechanisms in a rural site in China. They propose a self-amplifying feedback loop that link ammonia gas-particle conversion ratio with secondary inorganic aerosol. Overall, this paper makes a meaningful contribution to the haze formation mechanism in the rural agricultural areas in China. I favor its publication after the following issues are addressed.

Thanks for the positive comments.

1) Section 2.1 the authors have found the PM2.5 mass concentrations on Chongming site is higher than the urban (Pudong) site. Which fraction (sulfate, nitrate, ammonium or organics) of $PM_{2.5}$ mass is higher?

Thanks for the comment. In this study, the organic mass was not measured on Chongming site. The mass concentration of ammonium on Chongming (6.2±4.5 μg m^{-3}) is higher than that on Pudong (5.0 ±5.5 μg m^{-3}). The sulfate (6.5±4.9 μg m^{-3}) and nitrate (7.6±9.1 μg m^{-3}) concentration on Chongming is slightly lower than the level of sulfate (6.8±5.7 μg m^{-3}) and nitrate (8.9±11.3 μg m^{-3}) on Pudong.

2) Section 3.1 the authors straightly go to NH_3 levels in Chongming and its link to secondary inorganic aerosol. Since this article is about haze pollution, I would suggest them adding an overview section of the major PM2.5 species (NH4+, Na+, K+, Ca2+, Mg2+, Cl-, NO3-, and SO42-) to help the readers get a fully understanding about the typical air pollutants on the monitoring site.

Thanks for the comment. We have added a new section below in the Results and Discussion part to address the questions raised by the reviewer.

3.1 Overview of 1 year continuous measurements on Chongming

Figure 1 shows the time-series of hourly water-soluble $PM_{2.5}$ species during the study period. The mean concentration of NO_3^-, SO_4^{2-}, NH_4^+ and Cl^- over the entire study period was 8.4 μg m^{-3}, 6.3 μg m^{-3}, 6.3 μg m^{-3} and 1.2 μg m^{-3}. The haze period was defined as hourly averaged $PM_{2.5}$ mass loadings higher than 75 μg m^{-3} and the rest was non-haze period. Table 1 gives the statistical summary of major aerosols during the haze and non-haze period. Clearly, the mass concentration of major $PM_{2.5}$ species (NO_3^-, SO_4^{2-}, NH_4^+ and Cl^-) increased during the haze period compared to those during the non-haze period. However, the concentration of NH_3 showed no significant change during these two periods. The mean mass concentration of SNA (sulfate, nitrate, and ammonium) was 49.0 μg m^{-3}, contributing to 50.0 % of total $PM_{2.5}$ mass.

Table 1. Statistical summary on mass concentrations of $PM_{2.5}$ species and NH_3.

Unit: μg m^{-3}	$PM_{2.5}$	SO_4^{2-}	NO_3^-	Cl^-	NH_4^+	NH_3
non-haze	28.5 ± 16.9	5.6 ± 3.6	6.9 ± 6.6	1.1 ± 0.9	5.6 ± 3.3	32.2 ± 11.6
haze	98.3 ± 37.2	13.3 ± 7.7	23.1 ± 14.5	2.2 ± 1.9	13.2 ± 6.6	32.3 ± 13.5

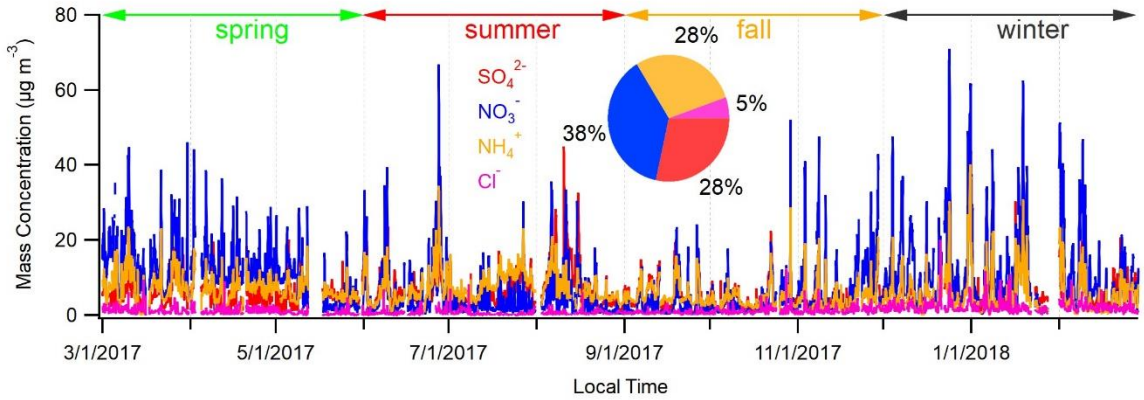

Figure 1: Time series of $PM_{2.5}$ species during the study period.

3) Section 3.2 ISORROPIA II has been used to predict the pH and aerosol water, however, the activity coefficient extracted from E-AIM IV was adopted. The authors should provide comparison of activity coefficients predicted from the two models (Peng et al., 2019, EST).

Thanks for the comment. We have re-calculated and re-plotted the S curve using activity coefficients taken from ISORROPIA II with the help of our co-author Dr. Hongyu Guo. For example, the following figure 6 has been replotted with $\frac{\gamma_{H^+}}{\gamma_{NH_4^+}}$ predicted by ISORROPIA II in the revision. Note the S curve only shifted to the right after the input of $\frac{\gamma_{H^+}}{\gamma_{NH_4^+}}$ changed from 2.4 ± 2.0 to 4.0 ± 2.6.

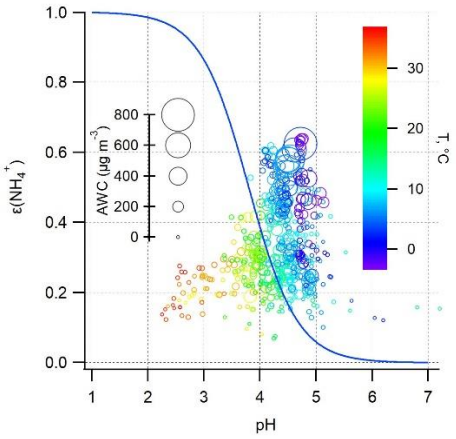

Figure 6: $\varepsilon(NH_4^+)$ as a function of pH during the haze period. The sizes of the void circles are scaled to AWC and colored by T. The blue curve was calculated based on the average T (10 °C), AWC (100 μg m^{-3}), and activity coefficients ratio of $\frac{\gamma_{H^+}}{\gamma_{NH_4^+}}$ respectively. The average $\frac{\gamma_{H^+}}{\gamma_{NH_4^+}}$ for the haze period is 4.0 ± 2.6 (±1σ).

4) Section 3.2 Lines 162-165, I suggest rephrasing the texts here.

Thanks for the comment. We noticed that the long range transport would not affect the equilibrium. After re-calculated the possible effect from organic mass, we have deleted these texts.

5) Section 3.2 I suggest the authors compare their ε(NH4+) S curve results with previous reports in other sites using the same methodology (e.g., Figure4 in Nah et al., 2018, ACP).

Thanks for the comment. A narrow range of aerosol water content (1 to 4 μg m^{-3}) and temperature (15 to 25 ◦C) in their ambient dataset was selected to be close to the input (AWC=2.5 μg m^{-3} and T = 20 ◦C) of analytically calculated S curves. However, in this study, the average AWC and T during the winter haze period was 100 μg m^{-3} and 10 ◦C, respectively. So a direct comparison to Nah et al.,

2018 should be discouraged. Using the same methodology, we picked a small range of AWC (80 to 120 μg m^{-3}) and T (8 to 12 ◦C) to be close to the average AWC (100 μg m^{-3}) and T (10 ◦C) during the haze period. We calculated the S curve of $\varepsilon(NH_4^+)$ with the average AWC and T and plot the data as below. Clearly, for the data points selected, there is roughly the same amount of spread compared to Nah et al., 2018.

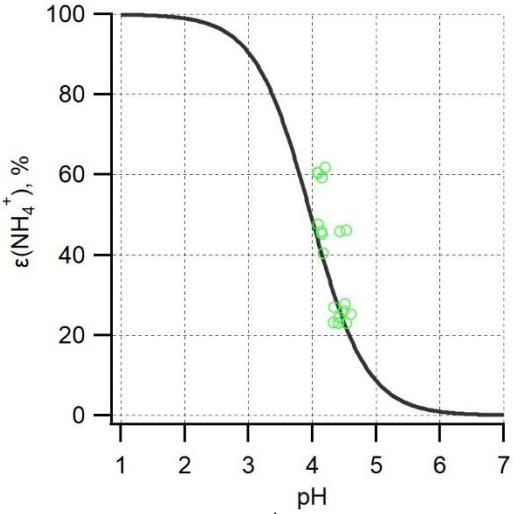

Figure R2: Analytically calculated S curves of $\varepsilon(NH_4^+)$ (Black curve) and measured $\varepsilon(NH_4^+)$ (void green circles) as a function of pH. A small range of AWC (80 to 120 μg m^{-3}) and T (8 to 12 ◦C) to be close to the average AWC (100 μg m^{-3}) and T (10 ◦C) was selected during the haze period. The S curve was calculated based on the average T (10 ℃), AWC (100 μg m^{-3}), and activity coefficients ratio of $\frac{\gamma_{H^+}}{\gamma_{NH_4^+}}$ (6.0) respectively. Note the average $\frac{\gamma_{H^+}}{\gamma_{NH_4^+}}$ for the selected ambient data we used to calculate the S curve is 6.0 not 4.0.

Reference

Battaglia Jr, M. A., Weber, R. J., Nenes, A., and Hennigan, C. J.: Effects of water-soluble organic carbon on aerosol pH, Atmos. Chem. Phys., 19, 14607-14620, 10.5194/acp-19-14607-2019, 2019.

Bougiatioti, A., Nikolaou, P., Stavroulas, I., Kouvarakis, G., Weber, R., Nenes, A., Kanakidou, M., and Mihalopoulos, N.: Particle water and pH in the eastern Mediterranean: source variability and implications for nutrient availability, Atmospheric Chemistry and Physics, 16, 4579-4591, 10.5194/acp-16-4579-2016, 2016.

Guo, H., Xu, L., Bougiatioti, A., Cerully, K. M., Capps, S. L., Hite Jr, J. R., Carlton, A. G., Lee, S. H., Bergin, M. H., Ng, N. L., Nenes, A., and Weber, R. J.: Fine-particle water and pH in the southeastern United States, Atmos. Chem. Phys., 15, 5211-5228, 10.5194/acp-15-5211-2015, 2015.

Guo, H., Liu, J., Froyd, K. D., Roberts, J. M., Veres, P. R., Hayes, P. L., Jimenez, J. L., Nenes, A., and Weber, R. J.: Fine particle pH and gas–particle phase partitioning of inorganic species in Pasadena, California, during the 2010 CalNex campaign, Atmos. Chem. Phys., 17, 5703-5719, 10.5194/acp-17-5703-2017, 2017.

Jin, X., Wang, Y., Li, Z., Zhang, F., Xu, W., Sun, Y., Fan, X., Chen, G., Wu, H., Ren, J., Wang, Q., and Cribb, M.: Significant contribution of organics to aerosol liquid water content in winter in Beijing, China, Atmos. Chem. Phys., 20, 901-914, 10.5194/acp-20-901-2020, 2020.

McNeill, V. F., Woo, J. L., Kim, D. D., Schwier, A. N., Wannell, N. J., Sumner, A. J., and Barakat, J. M.: Aqueous-Phase Secondary Organic Aerosol and Organosulfate Formation in Atmospheric Aerosols: A Modeling Study, Environmental Science & Technology, 46, 8075-8081, 10.1021/es3002986, 2012.

McNeill, V. F.: Aqueous Organic Chemistry in the Atmosphere: Sources and Chemical Processing of Organic Aerosols, Environmental Science & Technology, 49, 1237-1244, 10.1021/es5043707, 2015.

Pye, H. O. T., Nenes, A., Alexander, B., Ault, A. P., Barth, M. C., Clegg, S. L., Collett Jr, J. L., Fahey, K. M., Hennigan, C. J., Herrmann, H., Kanakidou, M., Kelly, J. T., Ku, I. T., McNeill, V. F., Riemer, N., Schaefer, T., Shi, G., Tilgner, A., Walker, J. T., Wang, T., Weber, R., Xing, J., Zaveri, R. A., and Zuend, A.: The acidity of atmospheric particles and clouds, Atmos. Chem. Phys., 20, 4809-4888, 10.5194/acp-20-4809-2020, 2020.

Tan, Y., Perri, M. J., Seitzinger, S. P., and Turpin, B. J.: Effects of Precursor Concentration and Acidic Sulfate in Aqueous Glyoxal−OH Radical Oxidation and Implications for Secondary Organic Aerosol, Environmental Science & Technology, 43, 8105-8112, 10.1021/es901742f, 2009.

Topping, D., Connolly, P., and McFiggans, G.: Cloud droplet number enhanced by co-condensation of organic vapours, Nature Geoscience, 6, 443-446, 10.1038/ngeo1809, 2013.

Wang, G., Zhang, F., Peng, J., Duan, L., Ji, Y., Marrero-Ortiz, W., Wang, J., Li, J., Wu, C., Cao, C., Wang, Y., Zheng, J., Secrest, J., Li, Y., Wang, Y., Li, H., Li, N., and Zhang, R.: Particle acidity and sulfate production during severe haze events in China cannot be reliably inferred by assuming a mixture of inorganic salts, Atmos. Chem. Phys., 18, 10123-10132, 10.5194/acp-18-10123-2018, 2018.

Xu, W., Han, T., Du, W., Wang, Q., Chen, C., Zhao, J., Zhang, Y., Li, J., Fu, P., Wang, Z., Worsnop, D. R., and Sun, Y.: Effects of Aqueous-Phase and Photochemical Processing on Secondary Organic Aerosol Formation and Evolution in Beijing, China, Environmental Science & Technology, 51, 762-770, 10.1021/acs.est.6b04498, 2017.

Importance of Gas-Particle Partitioning of Ammonia in Haze Formation in the Rural Agricultural Environment

Jian Xu[1], Jia Chen[1], Na Zhao[1], Guochen Wang[1], Guangyuan Yu[1], Hao Li[1], Juntao Huo[3], Yanfen Lin[3], Qingyan Fu[3], Hongyu Guo[4], Congrui Deng[1], Shan-Hu Lee[5], Jianmin Chen[1], Kan Huang[1,2]*

[1]Shanghai Key Laboratory of Atmospheric Particle Pollution and Prevention (LAP3), Department of Environmental Science and Engineering, Fudan University, Shanghai 200433, China
[2]Institute of Eco-Chongming (IEC), No.20 Cuiniao Road, Chen Jiazhen, Shanghai, China, 202162
[3]Shanghai Environmental Monitoring Center, Shanghai, 200030, China
[4]Cooperative Institute for Research in Environmental Sciences and Department of Chemistry, University of Colorado, Boulder, Colorado 80309, United States
[5]Department of Atmospheric Science, University of Alabama in Huntsville, Huntsville, AL 35758, USA

Correspondence to: Kan Huang (huangkan@fudan.edu.cn)

Abstract. Ammonia in the atmosphere is essential for the formation of fine particles that impact air quality and climate. Despite extensive prior research to disentangle the relationship between ammonia and haze pollution, the role of ammonia in haze formation in the high ammonia emitted regions is still not well understood. Aiming to better understand secondary inorganic aerosol (SNA) formation mechanisms under high ammonia conditions, one-year hourly measurement of water-soluble inorganic species (gas and particle) was conducted in a rural supersite in Shanghai. Exceedingly high levels of agricultural ammonia, constantly around 30 ug m^{-3}, were observed. We find that gas-particle partitioning of ammonia ($\varepsilon(NH_4^+)$), as opposed to ammonia concentrations, plays a critical role in SNA formation during the haze period. By assessing the effects of various parameters, including temperature (T), aerosol water content (AWC), aerosol pH, and activity coefficient, it seems that AWC plays predominant regulating roles for $\varepsilon(NH_4^+)$. We propose a self-amplifying feedback mechanism associated with $\varepsilon(NH_4^+)$ for the formation of SNA, which is consistent with diurnal variations of $\varepsilon(NH_4^+)$, AWC, and SNA. Our results imply that reduction of ammonia emissions alone may not reduce SNA effectively at least in rural agricultural sites in China.

1 Introduction

Gas-phase ammonia (NH_3) in the environment not only fuel the eutrophication and acidification of ecosystems, but also play key roles in atmospheric chemistry. NH_3 has been known to promote new particle formation both in the initial homogeneous nucleation and subsequent growth (Ball et al., 1999;Zhang et al., 2011;Coffman and Hegg, 1995;Kirkby et al., 2011). Prior studies suggest that the SO_2 oxidation can be enhanced by the presence of NH_3 (Turšič et al., 2004;Wang et al., 2016;Benner et al., 1992). High levels of NH_3 can also promote SOA formation (Na et al., 2007;Ortiz-Montalvo et al., 2013). As the main alkaline species in the atmosphere, NH_3 are expected to affect the acidity of clouds (Wells et al., 1998), fine particles (Liu et al., 2017;Guo et al., 2017b), and wet deposition (ApSimon et al., 1987) by neutralizing acidic species. The neutralized ammonium (NH_4^+) exclusively contribute to aerosol hygroscopicity especially in hazy periods (Liu et al., 2017;Ye et al., 2011). Serving as efficient catalysts for aerosol aldol condensation, ammonium has also been proved to contribute to radiative forcing (Noziere et al., 2010;Park et al., 2014). Most importantly, ammonium is among the major secondary inorganic aerosols (i.e., sulfate

Deleted: Ammonia Gas-Particle Conversion Ratio

Deleted: ammonia gas-particle conversion ratio

Deleted: ACR

Deleted: ACR

Deleted: ACR

Deleted: ACR

SO_4^{2-}, nitrate NO_3^-, and ammonium NH_4^+, denoted as SNA), which typically rivals the organics and can make up more than 50% of $PM_{2.5}$ mass loadings (Wang et al., 2015a;Sun et al., 2014;Huang et al., 2014;Plautz, 2018;Schiferl et al., 2014). Despite the significant importance of SNA in hazy periods, its formation mechanism responsible, particularly the role of NH_3, remains highly controversial. Cheng et al. (2016) and Wang et al. (2016), for example, suggested that the near-neutral acidity, resulting from the NH_3 rich atmosphere, is vital for SNA formation. While Liu et al. (2017) and Guo et al. (2017b) demonstrated that the close to neutral state is unlikely even under conditions of excess NH_3. These findings collectively imply that the fundamental role of NH_3 in regulating aerosol acidity is still ambiguous, thus altering the SNA formation mechanism (Seinfeld and Pandis, 2012).

NH_3 emission sources include agricultural practices, on-road vehicles(Chang et al., 2016;Sun et al., 2016) and biomass burning (Lamarque et al., 2010;Paulot et al., 2017). Recent field measurements and modeling works reveal that agricultural practices (i.e., animal manure and fertilizer application) contribute to 80-90% of total NH_3 emissions in China (Zhang et al., 2018;Kang et al., 2016;Huang et al., 2011). Globally, NH_3 emissions are projected to continue to rise along with increasing demand of chemical fertilizers due to the growing human population (Erisman et al., 2008;Stewart et al., 2005) and in part because limiting NH_3 emissions has not been targeted a priority in most countries. For example, even though stringent mitigation targets have been set for SO_2 and NO_x in China's 13th Five-Year Plan (2016-2020), slashing NH_3 emissions is not yet a prime concern in China. The sustained increase of NH_3 has been observed from the space (Warner et al., 2017) and reported to deflect the mitigation efforts of SO_2 and NO_x emissions in East China (Fu et al., 2017).

Although agricultural NH_3 emission has been the subject of extensive research, previous studies have focused on densely populated or urban areas, where NH_3 was mostly "aged" and transformed to NH_4^+ downwind (Chang et al., 2016). Varying in location and time, the typical mass concentrations of NH_3 are on the order of several micrograms per cubic meter(Yao et al., 2006;Gong et al., 2013;Robarge et al., 2002;Chang et al., 2016;Phan et al., 2013), with extremely high levels up to more than 20 μg m^{-3} in the rural area of North China Plain(Meng et al., 2018;Shen et al., 2011;Pan et al., 2018). Numerous studies highlighted the importance of NH_3 emissions from agricultural areas (Meng et al., 2018;Shen et al., 2011;Robarge et al., 2002;Wang et al., 2013;Nowak et al., 2012;Zhang et al., 2017;Warner et al., 2017), but the gas-particle conversion of agricultural NH_3 in rural regions and its subsequent impact on SNA formation, has scarcely been reported and remains poorly understood.

In this study, we provide observational constraints on the abnormally high agricultural NH_3 emission at a rural site. We report our findings on the influence of $\varepsilon(NH_4^+)$ on SNA formation and discuss the decisive factors driving the $\varepsilon(NH_4^+)$.

2 Methods

2.1 Observation site

Field measurements of gases and fine particles were conducted over the course of a year from March 2017 to February 2018 at the Dongtan Wetland Park (31°32′ N, 121°58′ E; altitude: 12 m a.s.l.), which is approximately 50 km northeast of downtown Shanghai. The sampling site, illustrated in Figure 1, was located on the east side of the Chongming island, which is the largest eco-friendly island in China and the least developed district of Shanghai. The

annual mean relative humidity (RH) is 78% ± 19% and the yearly mean temperature (T) is 16.3 ± 9.9°C. Although Chongming shares limited industrial and vehicle emissions compared to urban Shanghai, the level of fine particles on this island is slightly higher than the urban site (Figure S1). The overuse of nitrogen fertilizer has long been a large agricultural source of NH_3 emissions in China (Fan et al., 2011), with an increasing use especially in East-Central China (Yang and Fang, 2015), where rice/wheat intercropping (similar to those in Chongming) was applied. Based on a 2011 agricultural NH_3 emission inventory in Shanghai, Chongming has the largest nitrogen fertilizer consumption among all the districts in Shanghai (Fang et al., 2015). According to the Multi-resolution Emission Inventory for China (MEIC, www.meicmodel.org) in 2016, nearly 94% of NH_3 in Chongming came from the agricultural sector, accounting for 14% of the total NH_3 emissions in Shanghai. In comparison, Chongming contributes only 6% and 5% of the total NO_x and SO_2 emissions in Shanghai, respectively (Table S1). With the most intensive agriculture and 34% of arable farmland area in Shanghai (Wen et al., 2011), atmospheric ammonium aerosols over the Chongming island are mostly of agricultural origin. Therefore, this site is ideal for investigating the role of agricultural emissions of NH_3 in haze formation.

2.2 Measurements

Water-soluble samples of both gases (NH_3, SO_2, HCl, HNO_2, and HNO_3) and particles (NH_4^+, Na^+, K^+, Ca^{2+}, Mg^{2+}, Cl^-, NO_3^-, and SO_4^{2-}) were measured hourly using MARGA (Monitor for AeRosols and Gases in Air, ADI 2080, Metrohm Applikon B.V., Netherlands). Online sampling was conducted from March 2017 to February 2018 following the description in Kong et al. (2014). Briefly, air was drawn into a $PM_{2.5}$ cyclone inlet with a flow rate of 1 $m^3\ h^{-1}$ and passed through either a wet rotating denuder (gases) or a steam jet aerosol collector (aerosols). Subsequently, the aqueous samples were analyzed with ion chromatography. Meanwhile, mass loadings of $PM_{2.5}$ was determined by a Tapered Element Oscillating Microbalance coupled with Filter Dynamic Measurement System (TEOM 1405-F). The QA/QC of these instruments were managed by professional staff in Shanghai Environmental Monitoring Center (SEMC) according to the Technical Guideline of Automatic Stations of Ambient Air Quality in Shanghai (HJ/T193-2005).

2.3 ISORROPIA-II modelling

The thermodynamic model ISORROPIA II (Fountoukis and Nenes, 2007) was used to predict the aerosol water content and pH. ISORROPIA was constrained in forward metastable mode by hourly mean measurements of Na^+, K^+, Mg^{2+}, Ca^{2+}, SO_4^{2-}, NH_3, NH_4^+, HNO_3, NO_3^-, HCl, and Cl^-, along with RH and T. The molality based pH was a default output in the model. The model showed a good performance when predicting NH_3-NH_4^+ partitioning (Figure S2).

3 Results and Discussion

3.1 Overview of 1 year continuous measurements at Chongming

Figure 2 shows the time-series of hourly water-soluble $PM_{2.5}$ species during the study period. The mean concentration of NO_3^-, SO_4^{2-}, NH_4^+ and Cl^- over the entire study period was 8.4 μg m^{-3}, 6.3 μg m^{-3}, 6.3 μg m^{-3} and

Deleted: average

Deleted: $PM_{2.5}$ and gaseous pollutants (SO_2, NO_2, O_3, and CO) were monitored by co-located instruments. M

Deleted: . SO_2 mass concentrations were analyzed by Pulsed Fluorescence SO_2 Analyzer (Thermo Fisher Scientific, Model 43i). NO_2 mass concentrations were analyzed by Chemiluminescence NO-NO_2-NO_x Analyzer (Thermo Fisher Scientific, Model 42i). O_3 mass concentrations were analyzed by UV Photometric Ozone Analyzer (Thermo Fisher Scientific, Model 49i). CO mass concentrations were analyzed by Gas Filter Correlation CO Analyzer (Thermo Fisher Scientific, Model 48i). The QA/QC of these instruments were

Deleted: average

Deleted: d

Formatted: Line spacing: 1.5 lines

1.2 μg m^{-3}. The haze period was defined as hourly mean $PM_{2.5}$ mass loadings higher than 75 μg m^{-3} and the rest was non-haze periods. Table 1 gives the statistical summary of major aerosols during the haze and non-haze period. Clearly, the mass concentration of major $PM_{2.5}$ species (NO_3^-, SO_4^{2-}, NH_4^+ and Cl^-) increased during the haze period compared to those during the non-haze period. However, the concentration of NH_3 showed no significant change during these two periods. The mean mass concentration of SNA (sulfate, nitrate, and ammonium) was 49.0 μg m^{-3}, contributing to about 50.0 % of total $PM_{2.5}$ mass.

3.2 NH_3 levels and its link to secondary inorganic aerosol

Figure 3 shows that the mean concentration of NH_3 at Chongming (CM: 17.0 ± 4.2 μg m^{-3}) was more than three times higher than an urban site in Shanghai (PD: 2.5 ± 0.9 μg m^{-3}) and a representative regional transport region (DL: 4.6 ± 2.0 μg m^{-3}) in the Yangtze River Delta. The level of NH_3 at Chongming was even close to that observed inside a typical dairy farm (JS: 19.4 ± 12.6 μg m^{-3}), which was dominated by livestock emissions. Thus, it is interesting to investigate how the formation of secondary inorganic aerosols is impacted by this abnormally high level of NH_3.

Figure 4 indicates the response of SNA (sulfate, nitrate, and ammonium) mass concentrations to NH_3 is nonlinear. Higher NH_3 sometimes correspond to even lower SNA mass concentrations. Statistically, the mean SNA concentration in each bin of NH_3 doesn't show significant difference. This is at odds with the traditional view that higher concentrations of precursors usually result in elevated inorganic aerosols (Nowak et al., 2010). Although the abundance of SNA is related to the alkaline gaseous precursor (e.g., NH_3), the ambient condition (e.g., RH and T), and acid precursors (i.e., SO_2 and NO_x) whether favor the conversion of precursors into particles or not is equally important, if not higher. For example, the urban areas show higher SNA levels than the rural region while lower NH_3 mixing ratio was observed (Wu et al., 2016;Wang et al., 2015b). Previous field measurements suggest that rural NH_4^+ levels were more sensitive to acidic gases than to the NH_3 availability (Shen et al., 2011;Robarge et al., 2002). Therefore, the level of NH_3 concentration is not the determining factor for the formation of secondary inorganic aerosols.

3.3 The role of $\varepsilon(NH_4^+)$

In this regard, we further investigate the relationship between the gas-particle partitioning of ammonia ($\varepsilon(NH_4^+)$, defined as the molar ratio between particle phase ammonia (NH_4^+) and total ammonia ($NH_x = NH_3+NH_4^+$)) and SNA during the haze period. The haze period is defined as hourly mean $PM_{2.5}$ mass loadings higher than 75 μg m^{-3}. As shown in Figure 5, it is obvious that SNA in $PM_{2.5}$ is almost linearly correlated with $\varepsilon(NH_4^+)$. Higher $\varepsilon(NH_4^+)$ results in higher SNA concentrations. In addition, under the same $\varepsilon(NH_4^+)$ conditions, higher NH_3 promotes stronger formation of SNA. Thus, NH_3 and $\varepsilon(NH_4^+)$ collectively determine the haze formation potential. The level of NH_3 can be regarded as a proxy of NH_3 emission intensity, which is source dependent. As for $\varepsilon(NH_4^+)$, it represents the relative abundance of gaseous NH_3 and particulate ammonium. The shift between the two phases is controlled by various factors such as the ambient environmental conditions. Previous study shows that elevated RH and acidic gas levels favor the shift of NH_3 towards the particulate phase at an urban site, thereby a lower

Formatted: Font: (Default) Times New Roman
Deleted: 1
Deleted: i
Deleted: is
Deleted: is
Deleted: average
Deleted: are
Deleted: 2
Deleted: ammonia gas-particle conversion ratio
Deleted: ammonia gas-particle conversion ratio
Deleted: ACR
Deleted: average
Deleted: d
Deleted: ACR
Deleted: ACR
Deleted: ACR
Deleted: ACR
Deleted: ACR

[NH_3]:[NH_4^+] ratio was observed (Wei et al., 2015). In this study, it is also observed that higher $\varepsilon(NH_4^+)$ values coincide with heightened RH, SO_2, and NO_x.

Based on the above results, elucidation of the driving factors determining $\varepsilon(NH_4^+)$ is of great importance to explore the formation mechanism of haze. Theoretically, $\varepsilon(NH_4^+)$ is determined by NH_3, NH_4^+, and the equilibrium between NH_3 and NH_4^+. Assuming NH_3 and NH_4^+ are in thermodynamic equilibrium, the following equation can be obtained.

$H^+ + NH_{3(g)} \leftrightarrow NH_4^+$ (R1)

The equilibrium constant $H^*_{NH_3}$ is equal to the Henry's constant of NH_3 divided by the acid dissociation constant for NH_4^+ (Clegg et al., 1998). $\varepsilon(NH_4^+)$ can be analytically calculated as detailed in Guo et al.(2017a) via the following equation:

$$\varepsilon(NH_4^+) = \frac{[NH_4^+]}{[NH_x]} \cong \frac{\frac{\gamma_{H^+}10^{-pH}}{\gamma_{NH_4^+}} H^*_{NH_3} W_i RT \times 0.987\times10^{-14}}{1+\frac{\gamma_{H^+}10^{-pH}}{\gamma_{NH_4^+}} H^*_{NH_3} W_i RT \times 0.987\times10^{-14}} \quad \text{(Eq. 1)}$$

here, $[NH_4^+]$ is the molar concentration of NH_4^+ (mole m^{-3}). γ is the activity coefficient, which is extracted from the ISORROPIA II model to account for the non-ideality solution effect. $H^*_{NH_3}$ (atm^{-1}) represents the molality-based equilibrium constant, which is T dependent and can be determined using equation (12) in Clegg et al.(1998). W_i ($\mu g\ m^{-3}$) is the aerosol water content predicted by ISORROPIA-II. R (J/mole/K) is the universal gas constant. T (K) is ambient temperature and 0.987×10^{-14} is the conversion multiplication factors from atm and μg to SI units.

In Figure 6, $\varepsilon(NH_4^+)$ curve (The "S" shape curve, referred to as "S Curve" hereafter) is plotted against pH based on the mean T (10°C), AWC (100 $\mu g\ m^{-3}$), and $\frac{\gamma_{H^+}}{\gamma_{NH_4^+}}$ (2.4) during the haze period. Observation-based $\varepsilon(NH_4^+)$ as a function of pH with varying T and AWC is also shown. Clearly, the observational $\varepsilon(NH_4^+)$ data points are relatively well constrained by the theoretical equation, suggestive of reasonable judgement that $\varepsilon(NH_4^+)$ is controlled by T, AWC, pH, and $\frac{\gamma_{H^+}}{\gamma_{NH_4^+}}$. Under the condition of mean pH (4.6 ± 0.3) during the winter haze period, the "S curve" derives $\varepsilon(NH_4^+)$ of 0.3, around 3/4 of the mean measured $\varepsilon(NH_4^+)$ (0.4 ± 0.1). Earlier works have also observed higher particle phase fraction than the henry's law constants predicted for water soluble aerosol components (Arellanes et al., 2006;Hennigan et al., 2008;Shen et al., 2018). Another possible factor contributing to the underestimation of $\varepsilon(NH_4^+)$ is the unaccounted effect from organic species, whose role in driving the SNA formation is thought to be significant (Silvern et al., 2017). The organics have been found to account for 35% of AWC in the southeast USA (Guo et al., 2015), thus $\varepsilon(NH_4^+)$ would be enhanced by including organic aerosol. Since the mass concentration of organic aerosol was not available in this study, we did a sensitivity analysis via increasing the AWC by 10, 20 to 90 $\mu g\ m^{-3}$ as shown in Figure 7. The pH was not re-calculated using the new AWC because the co-existed organic aerosol altered pH in a complex way (Battaglia Jr et al., 2019;Wang et al., 2018;Pye et al., 2020). For example, some organic acids increase aerosol acidity thus decrease pH, whereas organic basics (e.g., amines) raise aerosol pH. We found that the best agreement between the predicted and measured $\varepsilon(NH_4^+)$ was achieved when we increase the AWC by roughly 90 $\mu g\ m^{-3}$, suggesting a nearly 48% of AWC contributed by the

Deleted: E-AIM IV

Deleted: (Clegg et al., 1998a)

Deleted: ACR

Deleted: average

Deleted: ACR

Deleted: ACR

Deleted: ACR

Deleted: average

Deleted: ACR

Deleted: 2

Deleted: half

Deleted: average

Deleted: ACR

Deleted: Regional and long-range transport of aerosol pollutants from northern China during the cold season (Xu et al., 2018) may have increased NH_4^+, yet NH_3 remains little unaffected because of its limited transport distance (Asman et al., 1998). The transport effect cannot be predicted by the theoretical equation and this should partly explain the divergence between the calculated and observed ACR.

Deleted: ACR

Deleted: ACR

organics. This result falls in the range from a recent report in North China that organics contribute to 30 % ± 22% of AWC (Jin et al., 2020), and slightly higher than those southeastern United States sites that organic aerosol-related water accounting for about 29 to 39% of total water (Guo et al., 2015) and those in the eastern Mediterranean that about 27.5% of total aerosol water resulted from organics (Bougiatioti et al., 2016). To quantitatively determine which parameter dominates the $\varepsilon(NH_4^+)$, the impact on $\varepsilon(NH_4^+)$ from individual variable (i.e. T, AWC, pH, and $\frac{\gamma_{H^+}}{\gamma_{NH_4^+}}$) during the haze period in winter is assessed (Figure 8). From a theoretical perspective, the decrease of pH and T, and increase of AWC and $\frac{\gamma_{H^+}}{\gamma_{NH_4^+}}$ would raise $\varepsilon(NH_4^+)$. For instance, in summertime, the lower $\varepsilon(NH_4^+)$ (Figure 4) are mainly due to higher T that shift the equilibrium to the gas phase, thus higher NH_3 (40 ± 8 μg m^{-3}) while lower NH_4^+ was observed. Likewise, in wintertime, the lower T facilitates the residence of NH_4^+ in the particle phase than the gas phase (NH_3: 20 ± 4 μg m^{-3}), resulting in higher $\varepsilon(NH_4^+)$. On the basis of "S curve" (Figure 8), each 0.1 unit change of $\varepsilon(NH_4^+)$ can be caused by approximate 5 °C, 75 μg m^{-3}, 0.3, and 2 units change of T, AWC, pH, and $\frac{\gamma_{H^+}}{\gamma_{NH_4^+}}$, respectively. Actually, T, pH, and $\frac{\gamma_{H^+}}{\gamma_{NH_4^+}}$ are within a relatively narrow range during the winter haze period (Table 2), suggesting the variation of these parameters shouldn't result in the significant change of $\varepsilon(NH_4^+)$. On the contrary, AWC fluctuates greatly during the study period (Table 2). Therefore, AWC should be the key factor regulating $\varepsilon(NH_4^+)$. It is well established that AWC is a function of RH and atmospheric aerosol compositions (Pilinis et al., 1989;Wu et al., 2018;Nguyen et al., 2016;Hodas et al., 2014). AWC has also been known to promote secondary organic aerosol formation by providing aqueous medium for uptake of reactive gases, gas to particle partitioning, and the subsequent chemical processing (McNeill, 2015;McNeill et al., 2012;Tan et al., 2009;Xu et al., 2017b).

The winter haze pH in this study were ~3 units higher than that of the southeastern United States summer campaign (Nah et al., 2018;Guo et al., 2015;Guo et al., 2017a;Xu et al., 2017a), but close to that of 3.7 in rural Europe (Guo et al., 2018) and 4.2 in North China Plain (Liu et al., 2017), where NH_3-rich conditions are prevalent. AWC may act as the major factor, because greater AWC dilute the $[H^+]$ and raise the pH. The AWC during the haze period (82 ± 105 μg m^{-3}) were much higher than those during the non-haze period (32 ± 41 μg m^{-3}).

3.4 A possible self-amplifying feedback mechanism

Given that AWC is a function of RH and SNA, a conceptual model of how AWC control $\varepsilon(NH_4^+)$ can be illustrated by a self-amplifying feedback loop (Figure 9). Formation of SNA is initiated by gas-particle conversion of NH_3. Under certain meteorological conditions such as high RH and shallow planetary boundary layer, SNA is subject to uptake moisture and result in the increases of AWC. The enhanced aerosol water dilutes the vapor pressure of semi-volatile species (i.e., nitrate, ammonium and chloride) above the particle and driving semi-volatile species continue to condense (Topping et al., 2013). Based on the discussions above, the increase of AWC would further raise $\varepsilon(NH_4^+)$, leading to more efficient transformation of NH_3 as SNA.

Figure 10 shows the yearly mean diurnal variation of $\varepsilon(NH_4^+)$, AWC, SNA along with T and RH. Apparently, SNA tracked well with $\varepsilon(NH_4^+)$ and AWC, especially over nighttime. The not well-correlated track between SNA and

Deleted: ACR
Deleted: ACR
Deleted: 7
Deleted: ACR
Deleted: ACR
Deleted: ACR
Deleted: 7
Deleted: ACR
Deleted: 1
Deleted: ACR
Deleted: 1
Deleted: ACR
Deleted: 3
Deleted: ACR
Deleted: 8
Deleted: ACR
Deleted: 9
Deleted: average
Deleted: ACR
Deleted: ACR

AWC and $\varepsilon(NH_4^+)_r$ during the daytime (8:00-16:00) can be ascribed to the photochemical reactions that lead to SNA formation. The good correlation between SNA and AWC and $\varepsilon(NH_4^+)_r$ demonstrated in Figure 10 support the proposed self-amplifying feedback loop in SNA formation.

Deleted: ACR

Deleted: ACR

Deleted: f

Deleted: 9

4 Conclusion

Our results demonstrate that $\varepsilon(NH_4^+)$, rather than NH_3 concentrations, plays a critical role in driving haze formation in the agricultural NH_3 emitted regions. Based on the "S curve" calculation, we have unraveled that AWC is the major factor controlling $\varepsilon(NH_4^+)$. Upon analyzing the cross-correlations between AWC, $\varepsilon(NH_4^+)$ and SNA, we proposed a self-amplifying feedback mechanism of SNA formation that associated with AWC and $\varepsilon(NH_4^+)$. This positive feedback cycle is likely to occur in other rural regions, where high agricultural NH_3 emissions are prevalent. We have shown that high NH_3 concentrations may not necessarily lead to strong SNA formation, particularly in the agriculture intensive areas, e.g. the North China Plain (NCP) and the extensive farming lands in Eastern China where the high NH_3 levels are still unregulated and increasing (Meng et al., 2018;Warner et al., 2017). Although Liu et al.(2019) have predicted that $PM_{2.5}$ can be slashed by 11-17% when 50% reduction in NH_3 from the agricultural sector and 15% mitigation of NO_x and SO_2 emissions was achieved, a recent study has demonstrated that only when aerosol pH drops below 3.0, the NH_3 reduction would have expected mitigation effects (Guo et al., 2018). The winter haze pH (4.6 ± 0.3) in this study was mostly between 4-5. Our results thus imply that NH_3 only may not be an effective solution to tackle air pollution in these regions.

Data availability.

The data presented in this paper are available upon request from the corresponding author (huangkan@fudan.edu.cn).

Author contributions.

JX and KH conceived the study. JX, JC, and KH performed data analysis and wrote the paper. All authors contributed to the review of the manuscript.

Competing interests.

The authors declare that they have no conflict of interest.

Acknowledgements

The authors acknowledge support of the National Science Foundation of China (No. 91644105), the National Key R&D Program of China (2018YFC0213105), and the Natural Science Foundation of Shanghai (19ZR1421100). Jian Xu acknowledge project funded by China Postdoctoral Science Foundation (2019M651365).

References

ApSimon, H. M., Kruse, M., and Bell, J. N. B.: Ammonia emissions and their role in acid deposition, Atmospheric Environment, 21, 1939-1946, 10.1016/0004-6981(87)90154-5, 1987.

Arellanes, C., Paulson, S. E., Fine, P. M., and Sioutas, C.: Exceeding of Henry's Law by Hydrogen Peroxide Associated with Urban Aerosols, Environmental Science & Technology, 40, 4859-4866, 10.1021/es0513786, 2006.

Ball, S. M., Hanson, D. R., Eisele, F. L., and McMurry, P. H.: Laboratory studies of particle nucleation: Initial results for H_2SO_4, H_2O, and NH_3 vapors, Journal of Geophysical Research: Atmospheres, 104, 23709-23718, doi:10.1029/1999JD900411, 1999.

Battaglia Jr, M. A., Weber, R. J., Nenes, A., and Hennigan, C. J.: Effects of water-soluble organic carbon on aerosol pH, Atmos. Chem. Phys., 19, 14607-14620, 10.5194/acp-19-14607-2019, 2019.

Benner, W. H., Ogorevc, B., and Novakov, T.: Oxidation of SO_2 in thin water films containing NH_3, Atmospheric Environment. Part A. General Topics, 26, 1713-1723, 10.1016/0960-1686(92)90069-W, 1992.

Bougiatioti, A., Nikolaou, P., Stavroulas, I., Kouvarakis, G., Weber, R., Nenes, A., Kanakidou, M., and Mihalopoulos, N.: Particle water and pH in the eastern Mediterranean: source variability and implications for nutrient availability, Atmospheric Chemistry and Physics, 16, 4579-4591, 10.5194/acp-16-4579-2016, 2016.

Chang, Y., Zou, Z., Deng, C., Huang, K., Collett, J. L., Lin, J., and Zhuang, G.: The importance of vehicle emissions as a source of atmospheric ammonia in the megacity of Shanghai, Atmospheric Chemistry and Physics, 16, 3577-3594, 10.5194/acp-16-3577-2016, 2016.

Cheng, Y., Zheng, G., Wei, C., Mu, Q., Zheng, B., Wang, Z., Gao, M., Zhang, Q., He, K., Carmichael, G., Pöschl, U., and Su, H.: Reactive nitrogen chemistry in aerosol water as a source of sulfate during haze events in China, Science Advances, 2, e1601530, 10.1126/sciadv.1601530, 2016.

Clegg, S. L., Brimblecombe, P., and Wexler, A. S.: Thermodynamic Model of the System H^+–NH_4^+–SO_4^{2-}–NO_3^-–H_2O at Tropospheric Temperatures, The Journal of Physical Chemistry A, 102, 2137-2154, 10.1021/jp973042r, 1998.

Coffman, D. J., and Hegg, D. A.: A preliminary study of the effect of ammonia on particle nucleation in the marine boundary layer, Journal of Geophysical Research: Atmospheres, 100, 7147-7160, 10.1029/94JD03253, 1995.

Erisman, J. W., Sutton, M. A., Galloway, J., Klimont, Z., and Winiwarter, W.: How a century of ammonia synthesis changed the world, Nature Geoscience, 1, 636-639, 10.1038/ngeo325, 2008.

Fan, M., Shen, J., Yuan, L., Jiang, R., Chen, X., Davies, W. J., and Zhang, F.: Improving crop productivity and resource use efficiency to ensure food security and environmental quality in China, Journal of Experimental Botany, 63, 13-24, 10.1093/jxb/err248, 2011.

Fang, X., Shen, G., Xu, C., Qian, X., Li, J., Zhao, Z., Yu, S., and Zhu, C.: Agricultural ammonia emission inventory and its distribution characteristics in Shanghai, Acta Agriculturae Zhejiangensis, 27, 2177-2185 [In Chinese], 2015.

Fountoukis, C., and Nenes, A.: ISORROPIA II: a computationally efficient thermodynamic equilibrium model for K^+–Ca^{2+}–Mg^{2+}–NH_4^+–Na^+–SO_4^{2-}–NO_3^-–Cl^-–H_2O aerosols, Atmos. Chem. Phys., 7, 4639-4659, 10.5194/acp-7-4639-2007, 2007.

Fu, X., Wang, S., Xing, J., Zhang, X., Wang, T., and Hao, J.: Increasing Ammonia Concentrations Reduce the Effectiveness of Particle Pollution Control Achieved via SO_2 and NO_X Emissions Reduction in East China, Environmental Science & Technology Letters, 4, 221-227, 10.1021/acs.estlett.7b00143, 2017.

Gong, L., Lewicki, R., Griffin, R. J., Tittel, F. K., Lonsdale, C. R., Stevens, R. G., Pierce, J. R., Malloy, Q. G. J., Travis, S. A., Bobmanuel, L. M., Lefer, B. L., and Flynn, J. H.: Role of atmospheric ammonia in particulate matter formation in Houston during summertime, Atmospheric Environment, 77, 893-900, 10.1016/j.atmosenv.2013.04.079, 2013.

Guo, H., Xu, L., Bougiatioti, A., Cerully, K. M., Capps, S. L., Hite Jr, J. R., Carlton, A. G., Lee, S. H., Bergin, M. H., Ng, N. L., Nenes, A., and Weber, R. J.: Fine-particle water and pH in the southeastern United States, Atmos. Chem. Phys., 15, 5211-5228, 10.5194/acp-15-5211-2015, 2015.

Guo, H., Liu, J., Froyd, K. D., Roberts, J. M., Veres, P. R., Hayes, P. L., Jimenez, J. L., Nenes, A., and Weber, R. J.: Fine particle pH and gas–particle phase partitioning of inorganic species in Pasadena, California, during the 2010 CalNex campaign, Atmos. Chem. Phys., 17, 5703-5719, 10.5194/acp-17-5703-2017, 2017a.

Guo, H., Weber, R. J., and Nenes, A.: High levels of ammonia do not raise fine particle pH sufficiently to yield nitrogen oxide-dominated sulfate production, Scientific Reports, 7, 12109, 10.1038/s41598-017-11704-0, 2017b.

Guo, H., Otjes, R., Schlag, P., Kiendler-Scharr, A., Nenes, A., and Weber, R. J.: Effectiveness of ammonia reduction on control of fine particle nitrate, Atmos. Chem. Phys., 18, 12241-12256, 10.5194/acp-18-12241-2018, 2018.

Hennigan, C. J., Bergin, M. H., Dibb, J. E., and Weber, R. J.: Enhanced secondary organic aerosol formation due to water uptake by fine particles, Geophysical Research Letters, 35, L18801, 10.1029/2008GL035046, 2008.

Hodas, N., Sullivan, A. P., Skog, K., Keutsch, F. N., Collett, J. L., Decesari, S., Facchini, M. C., Carlton, A. G., Laaksonen, A., and Turpin, B. J.: Aerosol Liquid Water Driven by Anthropogenic Nitrate: Implications for Lifetimes of Water-Soluble Organic Gases and Potential for Secondary Organic Aerosol Formation, Environmental Science & Technology, 48, 11127-11136, 10.1021/es5025096, 2014.

Huang, C., Chen, C. H., Li, L., Cheng, Z., Wang, H. L., Huang, H. Y., Streets, D. G., Wang, Y. J., Zhang, G. F., and Chen, Y. R.: Emission inventory of anthropogenic air pollutants and VOC species in the Yangtze River Delta region, China, Atmos. Chem. Phys., 11, 4105-4120, 10.5194/acp-11-4105-2011, 2011.
Huang, R.-J., Zhang, Y., Bozzetti, C., Ho, K.-F., Cao, J.-J., Han, Y., Daellenbach, K. R., Slowik, J. G., Platt, S. M., Canonaco, F., Zotter, P., Wolf, R., Pieber, S. M., Bruns, E. A., Crippa, M., Ciarelli, G., Piazzalunga, A., Schwikowski, M., Abbaszade, G., Schnelle-Kreis, J., Zimmermann, R., An, Z., Szidat, S., Baltensperger, U., Haddad, I. E., and Prevot, A. S. H.: High secondary aerosol contribution to particulate pollution during haze events in China, Nature, 514, 218-222, 10.1038/nature13774, 2014.
Jin, X., Wang, Y., Li, Z., Zhang, F., Xu, W., Sun, Y., Fan, X., Chen, G., Wu, H., Ren, J., Wang, Q., and Cribb, M.: Significant contribution of organics to aerosol liquid water content in winter in Beijing, China, Atmos. Chem. Phys., 20, 901-914, 10.5194/acp-20-901-2020, 2020.
Kang, Y., Liu, M., Song, Y., Huang, X., Yao, H., Cai, X., Zhang, H., Kang, L., Liu, X., Yan, X., He, H., Zhang, Q., Shao, M., and Zhu, T.: High-resolution ammonia emissions inventories in China from 1980 to 2012, Atmos. Chem. Phys., 16, 2043-2058, 10.5194/acp-16-2043-2016, 2016.
Kirkby, J., Curtius, J., Almeida, J., Dunne, E., Duplissy, J., Ehrhart, S., Franchin, A., Gagné, S., Ickes, L., Kürten, A., Kupc, A., Metzger, A., Riccobono, F., Rondo, L., Schobesberger, S., Tsagkogeorgas, G., Wimmer, D., Amorim, A., Bianchi, F., Breitenlechner, M., David, A., Dommen, J., Downard, A., Ehn, M., Flagan, R. C., Haider, S., Hansel, A., Hauser, D., Jud, W., Junninen, H., Kreissl, F., Kvashin, A., Laaksonen, A., Lehtipalo, K., Lima, J., Lovejoy, E. R., Makhmutov, V., Mathot, S., Mikkilä, J., Minginette, P., Mogo, S., Nieminen, T., Onnela, A., Pereira, P., Petäjä, T., Schnitzhofer, R., Seinfeld, J. H., Sipilä, M., Stozhkov, Y., Stratmann, F., Tomé, A., Vanhanen, J., Viisanen, Y., Vrtala, A., Wagner, P. E., Walther, H., Weingartner, E., Wex, H., Winkler, P. M., Carslaw, K. S., Worsnop, D. R., Baltensperger, U., and Kulmala, M.: Role of sulphuric acid, ammonia and galactic cosmic rays in atmospheric aerosol nucleation, Nature, 476, 429, 10.1038/nature10343, 2011.
Kong, L., Yang, Y., Zhang, S., Zhao, X., Du, H., Fu, H., Zhang, S., Cheng, T., Yang, X., and Chen, J.: Observations of linear dependence between sulfate and nitrate in atmospheric particles, Journal of Geophysical Research: Atmospheres, 119, 341-361, 10.1002/2013JD020222, 2014.
Lamarque, J. F., Bond, T. C., Eyring, V., Granier, C., Heil, A., Klimont, Z., Lee, D., Liousse, C., Mieville, A., Owen, B., Schultz, M. G., Shindell, D., Smith, S. J., Stehfest, E., Van Aardenne, J., Cooper, O. R., Kainuma, M., Mahowald, N., McConnell, J. R., Naik, V., Riahi, K., and van Vuuren, D. P.: Historical (1850–2000) gridded anthropogenic and biomass burning emissions of reactive gases and aerosols: methodology and application, Atmos. Chem. Phys., 10, 7017-7039, 10.5194/acp-10-7017-2010, 2010.
Liu, M., Song, Y., Zhou, T., Xu, Z., Yan, C., Zheng, M., Wu, Z., Hu, M., Wu, Y., and Zhu, T.: Fine particle pH during severe haze episodes in northern China, Geophysical Research Letters, 44, 5213-5221, 10.1002/2017GL073210, 2017.
Liu, M., Huang, X., Song, Y., Tang, J., Cao, J., Zhang, X., Zhang, Q., Wang, S., Xu, T., Kang, L., Cai, X., Zhang, H., Yang, F., Wang, H., Yu, J. Z., Lau, A. K. H., He, L., Huang, X., Duan, L., Ding, A., Xue, L., Gao, J., Liu, B., and Zhu, T.: Ammonia emission control in China would mitigate haze pollution and nitrogen deposition, but worsen acid rain, Proceedings of the National Academy of Sciences, 116, 7760-7765, 10.1073/pnas.1814880116, 2019.
McNeill, V. F., Woo, J. L., Kim, D. D., Schwier, A. N., Wannell, N. J., Sumner, A. J., and Barakat, J. M.: Aqueous-Phase Secondary Organic Aerosol and Organosulfate Formation in Atmospheric Aerosols: A Modeling Study, Environmental Science & Technology, 46, 8075-8081, 10.1021/es3002986, 2012.
McNeill, V. F.: Aqueous Organic Chemistry in the Atmosphere: Sources and Chemical Processing of Organic Aerosols, Environmental Science & Technology, 49, 1237-1244, 10.1021/es5043707, 2015.
Meng, Z., Xu, X., Lin, W., Ge, B., Xie, Y., Song, B., Jia, S., Zhang, R., Peng, W., Wang, Y., Cheng, H., Yang, W., and Zhao, H.: Role of ambient ammonia in particulate ammonium formation at a rural site in the North China Plain, Atmos. Chem. Phys., 18, 167-184, 10.5194/acp-18-167-2018, 2018.
Na, K., Song, C., Switzer, C., and Cocker, D. R.: Effect of Ammonia on Secondary Organic Aerosol Formation from α-Pinene Ozonolysis in Dry and Humid Conditions, Environmental Science & Technology, 41, 6096-6102, 10.1021/es061956y, 2007.
Nah, T., Guo, H., Sullivan, A. P., Chen, Y., Tanner, D. J., Nenes, A., Russell, A., Ng, N. L., Huey, L. G., and Weber, R. J.: Characterization of aerosol composition, aerosol acidity, and organic acid partitioning at an agriculturally intensive rural southeastern US site, Atmos. Chem. Phys., 18, 11471-11491, 10.5194/acp-18-11471-2018, 2018.
Nguyen, T. K. V., Zhang, Q., Jimenez, J. L., Pike, M., and Carlton, A. G.: Liquid Water: Ubiquitous Contributor to Aerosol Mass, Environmental Science & Technology Letters, 3, 257-263, 10.1021/acs.estlett.6b00167, 2016.
Nowak, J. B., Neuman, J. A., Bahreini, R., Brock, C. A., Middlebrook, A. M., Wollny, A. G., Holloway, J. S., Peischl, J., Ryerson, T. B., and Fehsenfeld, F. C.: Airborne observations of ammonia and ammonium nitrate formation over Houston, Texas, Journal of Geophysical Research: Atmospheres, 115, D22304, 10.1029/2010JD014195, 2010.
Nowak, J. B., Neuman, J. A., Bahreini, R., Middlebrook, A. M., Holloway, J. S., McKeen, S. A., Parrish, D. D., Ryerson, T. B., and Trainer, M.: Ammonia sources in the California South Coast Air Basin and their impact on ammonium nitrate formation, Geophysical Research Letters, 39, L07804, 10.1029/2012GL051197, 2012.
Noziere, B., Dziedzic, P., and Cordova, A.: Inorganic ammonium salts and carbonate salts are efficient catalysts for aldol condensation in atmospheric aerosols, Physical Chemistry Chemical Physics, 12, 3864-3872, 10.1039/B924443C, 2010.

Ortiz-Montalvo, D. L., Häkkinen, S. A. K., Schwier, A. N., Lim, Y. B., McNeill, V. F., and Turpin, B. J.: Ammonium Addition (and Aerosol pH) Has a Dramatic Impact on the Volatility and Yield of Glyoxal Secondary Organic Aerosol, Environmental Science & Technology, 48, 255-262, 10.1021/es4035667, 2013.
Pan, Y., Tian, S., Zhao, Y., Zhang, L., Zhu, X., Gao, J., Huang, W., Zhou, Y., Song, Y., Zhang, Q., and Wang, Y.: Identifying Ammonia Hotspots in China Using a National Observation Network, Environmental Science & Technology, 52, 3926-3934, 10.1021/acs.est.7b05235, 2018.
Park, R. S., Lee, S., Shin, S. K., and Song, C. H.: Contribution of ammonium nitrate to aerosol optical depth and direct radiative forcing by aerosols over East Asia, Atmos. Chem. Phys., 14, 2185-2201, 10.5194/acp-14-2185-2014, 2014.
Paulot, F., Paynter, D., Ginoux, P., Naik, V., Whitburn, S., Van Damme, M., Clarisse, L., Coheur, P. F., and Horowitz, L. W.: Gas-aerosol partitioning of ammonia in biomass burning plumes: Implications for the interpretation of spaceborne observations of ammonia and the radiative forcing of ammonium nitrate, Geophysical Research Letters, 44, 8084-8093, 10.1002/2017GL074215, 2017.
Peng, G., Jie, W., Luyang, J., and Le, Y.: FROM-GLC 2015 v0.1, 10.6084/m9.figshare.5362774.v2, 2018.
Phan, N.-T., Kim, K.-H., Shon, Z.-H., Jeon, E.-C., Jung, K., and Kim, N.-J.: Analysis of ammonia variation in the urban atmosphere, Atmospheric Environment, 65, 177-185, 10.1016/j.atmosenv.2012.10.049, 2013.
Pilinis, C., Seinfeld, J. H., and Grosjean, D.: Water content of atmospheric aerosols, Atmospheric Environment, 23, 1601-1606, 10.1016/0004-6981(89)90419-8, 1989.
Plautz, J.: Piercing the haze, Science, 361, 1060, 2018.
Pye, H. O. T., Nenes, A., Alexander, B., Ault, A. P., Barth, M. C., Clegg, S. L., Collett Jr, J. L., Fahey, K. M., Hennigan, C. J., Herrmann, H., Kanakidou, M., Kelly, J. T., Ku, I. T., McNeill, V. F., Riemer, N., Schaefer, T., Shi, G., Tilgner, A., Walker, J. T., Wang, T., Weber, R., Xing, J., Zaveri, R. A., and Zuend, A.: The acidity of atmospheric particles and clouds, Atmos. Chem. Phys., 20, 4809-4888, 10.5194/acp-20-4809-2020, 2020.
Robarge, W. P., Walker, J. T., McCulloch, R. B., and Murray, G.: Atmospheric concentrations of ammonia and ammonium at an agricultural site in the southeast United States, Atmospheric Environment, 36, 1661-1674, 10.1016/S1352-2310(02)00171-1, 2002.
Schiferl, L. D., Heald, C. L., Nowak, J. B., Holloway, J. S., Neuman, J. A., Bahreini, R., Pollack, I. B., Ryerson, T. B., Wiedinmyer, C., and Murphy, J. G.: An investigation of ammonia and inorganic particulate matter in California during the CalNex campaign, Journal of Geophysical Research: Atmospheres, 119, 1883-1902, 10.1002/2013JD020765, 2014.
Seinfeld, J. H., and Pandis, S. N.: Atmospheric chemistry and physics: from air pollution to climate change, Wiley, 1232 pp., 2012.
Shen, H., Chen, Z., Li, H., Qian, X., Qin, X., and Shi, W.: Gas-Particle Partitioning of Carbonyl Compounds in the Ambient Atmosphere, Environmental Science & Technology, 52, 10997-11006, 10.1021/acs.est.8b01882, 2018.
Shen, J., Liu, X., Zhang, Y., Fangmeier, A., Goulding, K., and Zhang, F.: Atmospheric ammonia and particulate ammonium from agricultural sources in the North China Plain, Atmospheric Environment, 45, 5033-5041, 10.1016/j.atmosenv.2011.02.031, 2011.
Silvern, R. F., Jacob, D. J., Kim, P. S., Marais, E. A., Turner, J. R., Campuzano-Jost, P., and Jimenez, J. L.: Inconsistency of ammonium–sulfate aerosol ratios with thermodynamic models in the eastern US: a possible role of organic aerosol, Atmos. Chem. Phys., 17, 5107-5118, 10.5194/acp-17-5107-2017, 2017.
Stewart, W. M., Dibb, D. W., Johnston, A. E., and Smyth, T. J.: The Contribution of Commercial Fertilizer Nutrients to Food Production, Agronomy Journal, 97, 1-6, 10.2134/agronj2005.0001, 2005.
Sun, K., Tao, L., Miller, D. J., Pan, D., Golston, L. M., Zondlo, M. A., Griffin, R. J., Wallace, H. W., Leong, Y. J., Yang, M. M., Zhang, Y., Mauzerall, D. L., and Zhu, T.: Vehicle Emissions as an Important Urban Ammonia Source in the United States and China, Environmental Science & Technology, 10.1021/acs.est.6b02805, 2016.
Sun, Y., Jiang, Q., Wang, Z., Fu, P., Li, J., Yang, T., and Yin, Y.: Investigation of the sources and evolution processes of severe haze pollution in Beijing in January 2013, Journal of Geophysical Research: Atmospheres, 119, 4380-4398, 10.1002/2014JD021641, 2014.
Tan, Y., Perri, M. J., Seitzinger, S. P., and Turpin, B. J.: Effects of Precursor Concentration and Acidic Sulfate in Aqueous Glyoxal−OH Radical Oxidation and Implications for Secondary Organic Aerosol, Environmental Science & Technology, 43, 8105-8112, 10.1021/es901742f, 2009.
Topping, D., Connolly, P., and McFiggans, G.: Cloud droplet number enhanced by co-condensation of organic vapours, Nature Geoscience, 6, 443-446, 10.1038/ngeo1809, 2013.
Turšič, J., Berner, A., Podkrajšek, B., and Grgić, I.: Influence of ammonia on sulfate formation under haze conditions, Atmospheric Environment, 38, 2789-2795, 10.1016/j.atmosenv.2004.02.036, 2004.
Wang, G., Zhang, R., Gomez, M. E., Yang, L., Levy Zamora, M., Hu, M., Lin, Y., Peng, J., Guo, S., Meng, J., Li, J., Cheng, C., Hu, T., Ren, Y., Wang, Y., Gao, J., Cao, J., An, Z., Zhou, W., Li, G., Wang, J., Tian, P., Marrero-Ortiz, W., Secrest, J., Du, Z., Zheng, J., Shang, D., Zeng, L., Shao, M., Wang, W., Huang, Y., Wang, Y., Zhu, Y., Li, Y., Hu, J., Pan, B., Cai, L., Cheng, Y., Ji, Y., Zhang, F., Rosenfeld, D., Liss, P. S., Duce, R. A., Kolb, C. E., and Molina, M. J.: Persistent sulfate formation from London Fog to Chinese haze, Proceedings of the National Academy of Sciences, 113, 13630-13635, 10.1073/pnas.1616540113, 2016.
Wang, G., Zhang, F., Peng, J., Duan, L., Ji, Y., Marrero-Ortiz, W., Wang, J., Li, J., Wu, C., Cao, C., Wang, Y., Zheng, J., Secrest, J., Li, Y., Wang, Y., Li, H., Li, N., and Zhang, R.: Particle acidity and sulfate production during severe haze events in China cannot be reliably inferred by assuming a mixture of inorganic salts, Atmos. Chem. Phys., 18, 10123-10132, 10.5194/acp-18-10123-2018, 2018.

Wang, Q., Zhuang, G., Huang, K., Liu, T., Deng, C., Xu, J., Lin, Y., Guo, Z., Chen, Y., Fu, Q., Fu, J. S., and Chen, J.: Probing the severe haze pollution in three typical regions of China: Characteristics, sources and regional impacts, Atmospheric Environment, 120, 76-88, 10.1016/j.atmosenv.2015.08.076, 2015a.
Wang, S., Nan, J., Shi, C., Fu, Q., Gao, S., Wang, D., Cui, H., Saiz-Lopez, A., and Zhou, B.: Atmospheric ammonia and its impacts on regional air quality over the megacity of Shanghai, China, Scientific Reports, 5, 15842, 10.1038/srep15842, 2015b.
Wang, Y., Zhang, Q. Q., He, K., Zhang, Q., and Chai, L.: Sulfate-nitrate-ammonium aerosols over China: response to 2000–2015 emission changes of sulfur dioxide, nitrogen oxides, and ammonia, Atmos. Chem. Phys., 13, 2635-2652, 10.5194/acp-13-2635-2013, 2013.
Warner, J. X., Dickerson, R. R., Wei, Z., Strow, L. L., Wang, Y., and Liang, Q.: Increased atmospheric ammonia over the world's major agricultural areas detected from space, Geophysical Research Letters, 44, 2875-2884, 10.1002/2016GL072305, 2017.
Wei, L., Duan, J., Tan, J., Ma, Y., He, K., Wang, S., Huang, X., and Zhang, Y.: Gas-to-particle conversion of atmospheric ammonia and sampling artifacts of ammonium in spring of Beijing, Science China Earth Sciences, 58, 345-355, 10.1007/s11430-014-4986-1, 2015.
Wells, M., Choularton, T. W., and Bower, K. N.: A modelling study of the interaction of ammonia with cloud, Atmospheric Environment, 32, 359-363, 10.1016/S1352-2310(97)00199-4, 1998.
Wen, X., He, Z., and Zhang, Z.: Surveying and Evaluating of Land Environmental Quality and Monitoring of Basic Farmland Environmental Quality in Shanghai, Shanghai Land & Resources, 32, 8-13 [In Chinese], 2011.
Wu, Y., Gu, B., Erisman, J. W., Reis, S., Fang, Y., Lu, X., and Zhang, X.: $PM_{2.5}$ pollution is substantially affected by ammonia emissions in China, Environmental Pollution, 218, 86-94, 10.1016/j.envpol.2016.08.027, 2016.
Wu, Z., Wang, Y., Tan, T., Zhu, Y., Li, M., Shang, D., Wang, H., Lu, K., Guo, S., Zeng, L., and Zhang, Y.: Aerosol liquid water driven by anthropogenic inorganic salts: Implying its key role in haze formation over the North China Plain, Environmental Science & Technology Letters, 5, 160-166, 10.1021/acs.estlett.8b00021, 2018.
Xu, L., Guo, H., Weber, R. J., and Ng, N. L.: Chemical Characterization of Water-Soluble Organic Aerosol in Contrasting Rural and Urban Environments in the Southeastern United States, Environmental Science & Technology, 51, 78-88, 10.1021/acs.est.6b05002, 2017a.
Xu, W., Han, T., Du, W., Wang, Q., Chen, C., Zhao, J., Zhang, Y., Li, J., Fu, P., Wang, Z., Worsnop, D. R., and Sun, Y.: Effects of Aqueous-Phase and Photochemical Processing on Secondary Organic Aerosol Formation and Evolution in Beijing, China, Environmental Science & Technology, 51, 762-770, 10.1021/acs.est.6b04498, 2017b.
Yang, X., and Fang, S.: Practices, perceptions, and implications of fertilizer use in East-Central China, Ambio, 44, 647-652, 10.1007/s13280-015-0639-7, 2015.
Yao, X., Yan Ling, T., Fang, M., and Chan, C. K.: Comparison of thermodynamic predictions for in situ pH in PM2.5, Atmospheric Environment, 40, 2835-2844, 10.1016/j.atmosenv.2006.01.006, 2006.
Ye, X., Ma, Z., Zhang, J., Du, H., Chen, J., Chen, H., Yang, X., Gao, W., and Geng, F.: Important role of ammonia on haze formation in Shanghai, Environmental Research Letters, 6, 024019, 2011.
Zhang, L., Chen, Y., Zhao, Y., Henze, D. K., Zhu, L., Song, Y., Paulot, F., Liu, X., Pan, Y., Lin, Y., and Huang, B.: Agricultural ammonia emissions in China: reconciling bottom-up and top-down estimates, Atmos. Chem. Phys., 18, 339-355, 10.5194/acp-18-339-2018, 2018.
Zhang, R., Khalizov, A., Wang, L., Hu, M., and Xu, W.: Nucleation and growth of nanoparticles in the atmosphere, Chemical Reviews, 112, 1957-2011, 10.1021/cr2001756, 2011.
Zhang, X., Wu, Y., Liu, X., Reis, S., Jin, J., Dragosits, U., Van Damme, M., Clarisse, L., Whitburn, S., Coheur, P.-F., and Gu, B.: Ammonia Emissions May Be Substantially Underestimated in China, Environmental Science & Technology, 51, 12089-12096, 10.1021/acs.est.7b02171, 2017.

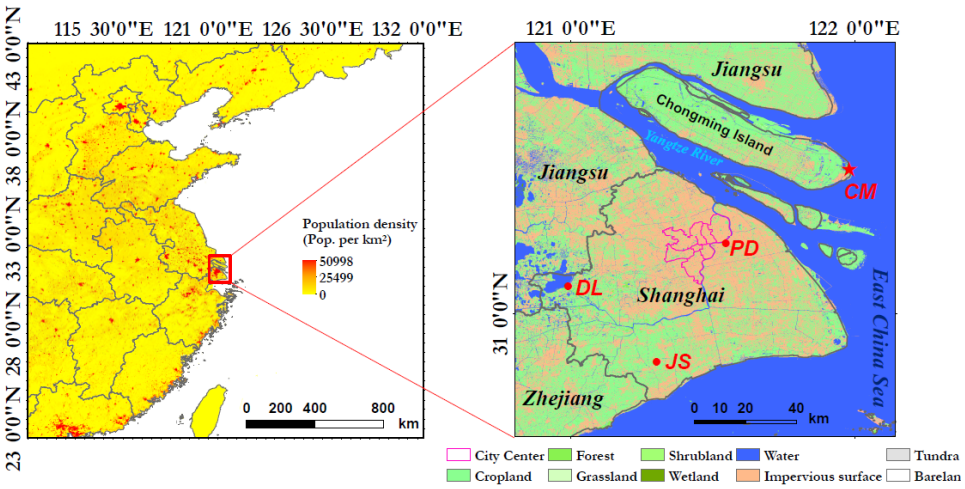

Figure 1: Location of the sampling site. Population density is color-coded in the left panel. The right panel shows the land cover in Shanghai (adapted from Peng et al.(2018)). CM (Chongming) is the sampling site on Chongming island. JS (Jinshan) represents the source emission from a dairy farm in rural Shanghai. DL (Dianshan Lake) represents a regional transport region in the Yangtze River Delta. PD (Pudong) represents the urban site.

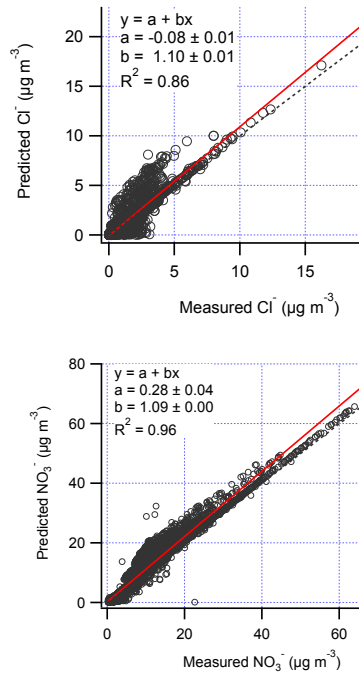

Deleted:
Figure 2: Comparison of predicted and measured Cl^-, NO_3^-, NH_3, NH_4^+. Orthogonal distance regression (ODR) fits with ±1σ are shown.

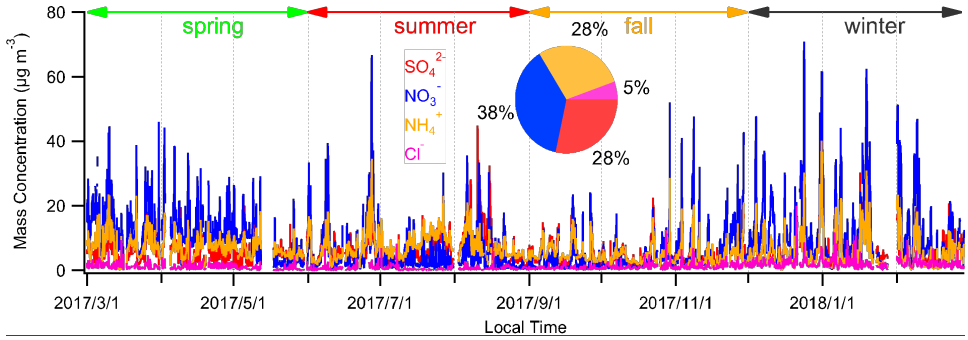

Figure 2: Time series of $PM_{2.5}$ species during the study period. The mass fraction of major $PM_{2.5}$ species is shown in the inserted pie chart.

Formatted: English (US)

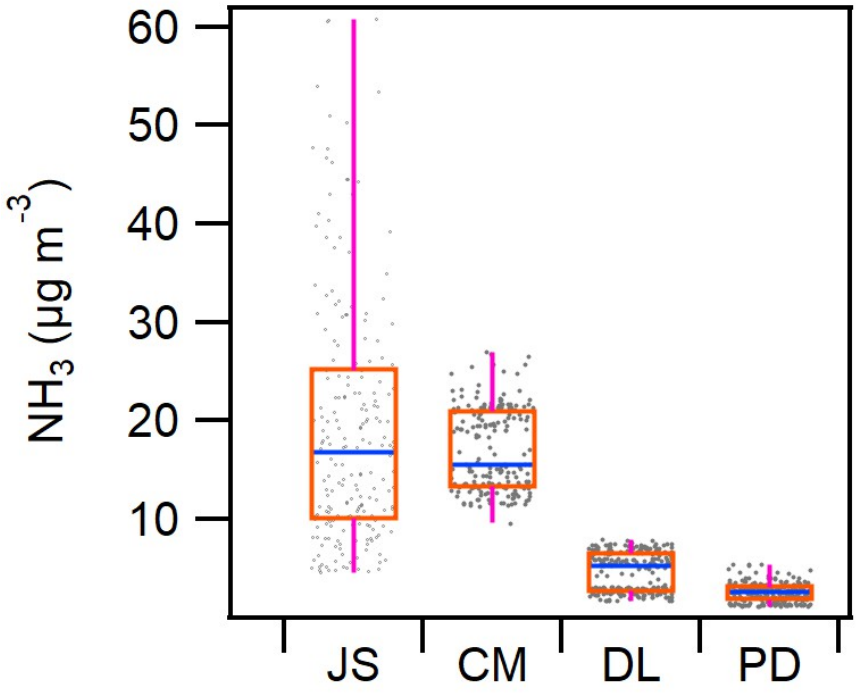

Figure 3: NH_3 at different sampling site over the same period (From Jan 18 to 27 of 2018). The locations of all sites are shown in Figure 1. Scattered dots indicate raw data points.

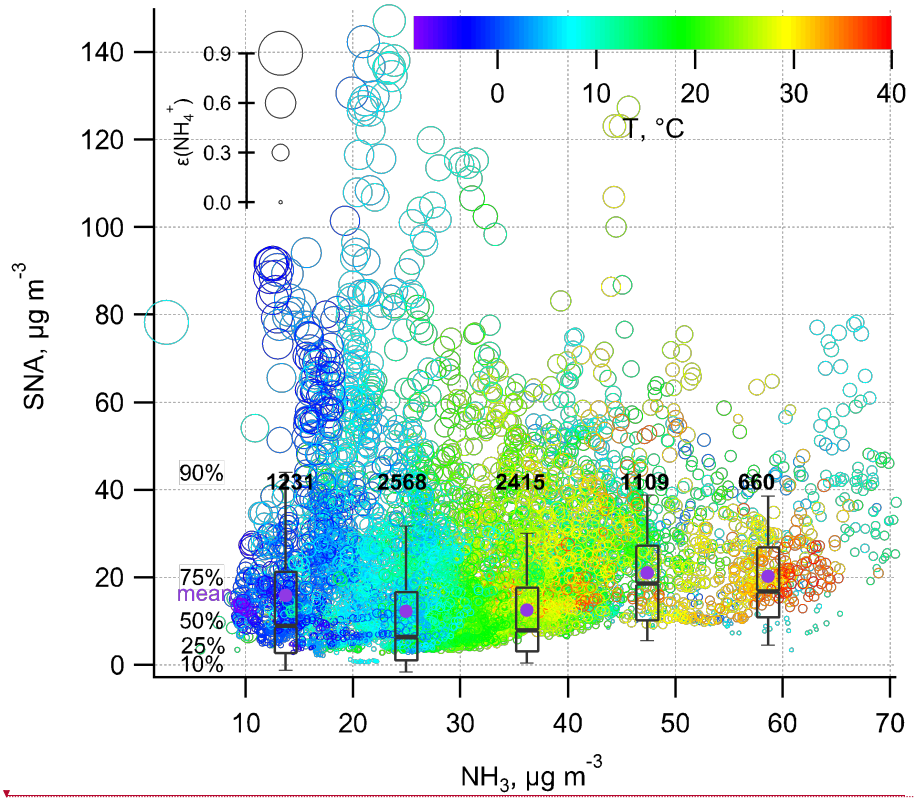

Figure 4: Secondary inorganic aerosol mass concentration in $PM_{2.5}$ (SNA refers to sulfate, nitrate, and ammonium) as a function of NH_3. The sizes of the void circles are scaled to the $\varepsilon(NH_4^+)$, and colored by T. The number of data points in each NH_3 concentration bin is also shown.

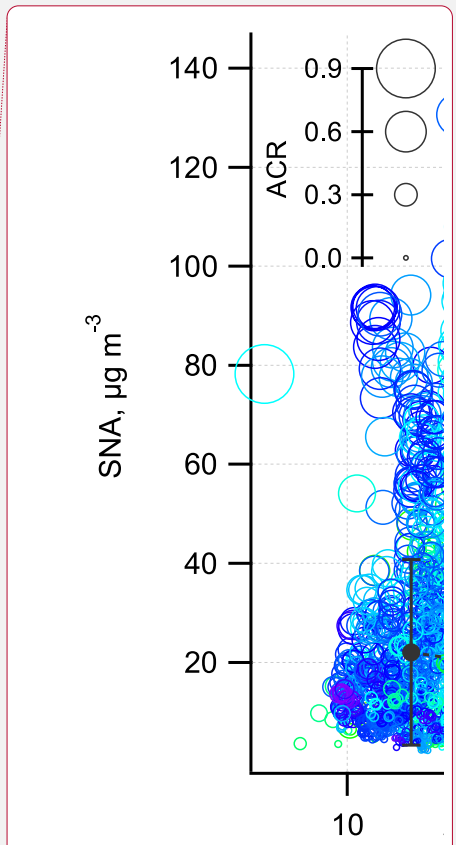

Deleted:

Deleted: ACR

Deleted: The SNA concentrations in black filled circles are binned and averaged according to the NH_3 mass concentration of each 10 μg m^{-3}. Error bars represent one standard deviation (±1σ).

Formatted: Subscript

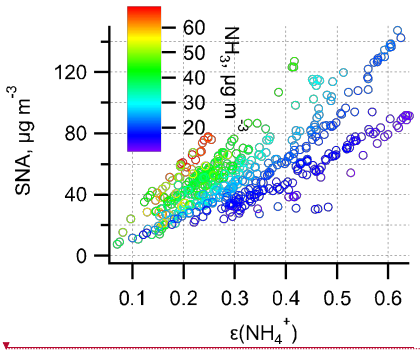

Figure 5: SNA mass concentration in $PM_{2.5}$ as a function of $\varepsilon(NH_4^+)$ during the haze period. The circles are colored by the NH_3 mass concentration.

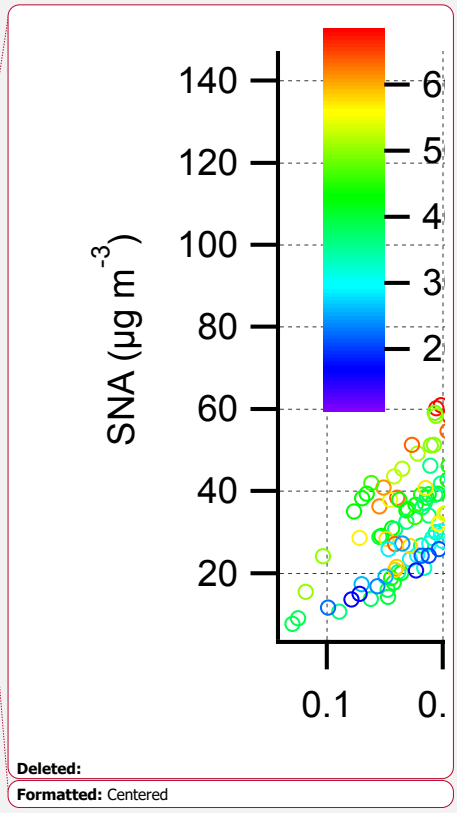

Deleted:

Formatted: Centered

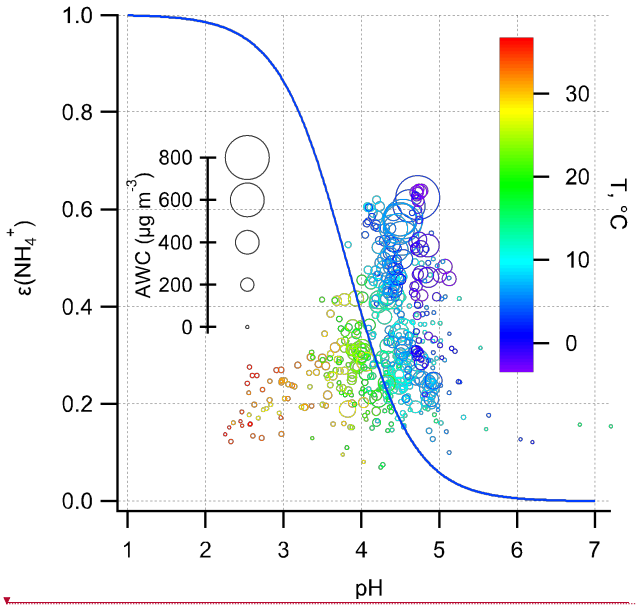

Figure 6: $\varepsilon(NH_4^+)$ **as a function of pH during the haze period. The sizes of the void circles are scaled to AWC and colored by T. The blue curve was calculated based on the mean T (10 °C), AWC (100 μg m^{-3}), and activity coefficients ratio of** $\frac{\gamma_{H^+}}{\gamma_{NH_4^+}}$ **respectively. The mean** $\frac{\gamma_{H^+}}{\gamma_{NH_4^+}}$ **for the haze period is 4.0 ± 2.6 (±1σ).**

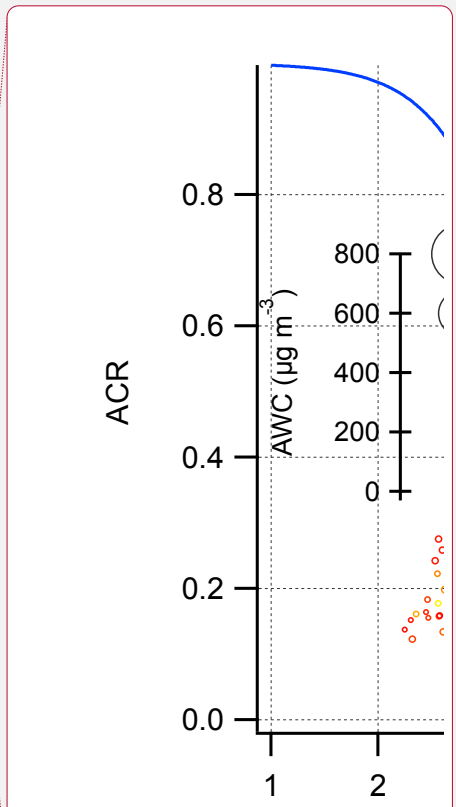

Deleted:

Formatted: Centered

Deleted: ACR

Deleted: average

Deleted: average

Deleted: 2.4

Deleted: 0

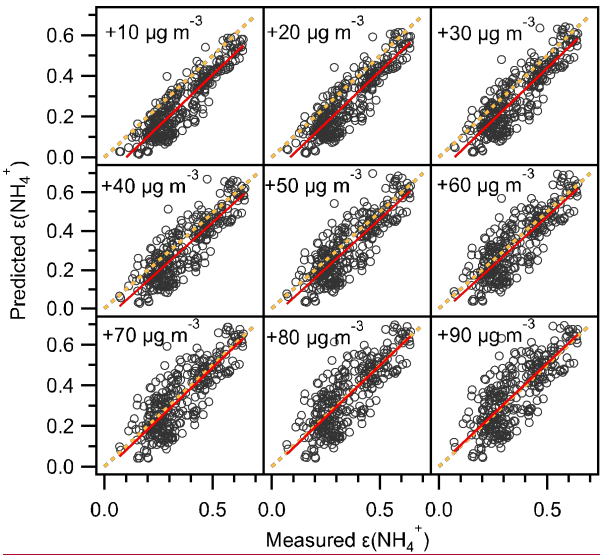

Figure 7: Comparison of predicted and measured $\varepsilon(NH_4^+)$. Note the predicted $\varepsilon(NH_4^+)$ was analytically calculated using the equation 2 with input (i.e., pH, AWC, $\frac{\gamma_{H^+}}{\gamma_{NH_4^+}}$) taken from ISORROPIA II prediction and the AWC has been increased by 10, 20 to 90 µg m^{-3} while other inputs fixed. Orthogonal distance regression (ODR) fits line (red) and y=x line (dashed orange) was shown for the clarity of the figure.

Formatted: Centered

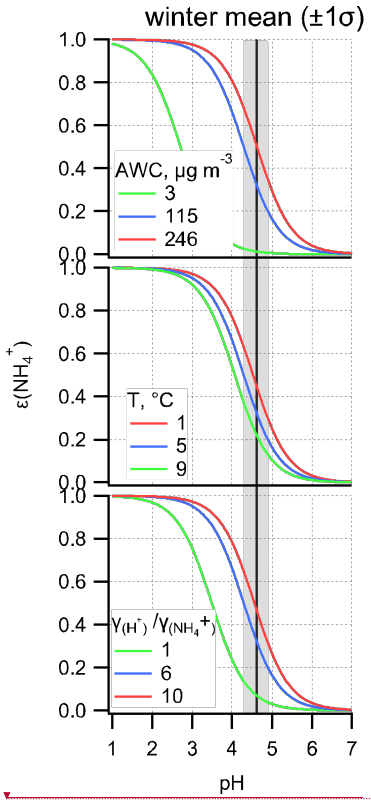

Figure 8: $\varepsilon(NH_4^+)$ **as a function of pH during the winter haze period. Other variables are held constant at the mean value during the winter haze period, while varying only the AWC, T, activity coefficients ratio of** $\frac{\gamma_{H^+}}{\gamma_{NH_4^+}}$**, respectively. Shaded dark areas indicate the winter haze mean pH together with one standard deviation (± 1σ). The areas between the green and red line represent the curve corresponding to mean ± 1σ, note that for AWC mean - 1σ yield a negative value, thus the minimum mass concentration (3 µg m^{-3}) was used.**

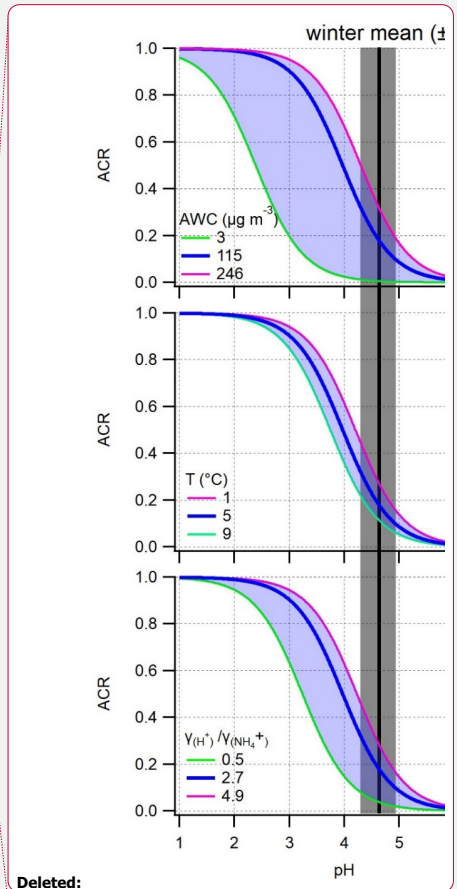

Deleted:
Formatted: Centered
Deleted: 7
Deleted: ACR
Deleted: average
Deleted: average
Deleted: Shaded blue
Deleted: average
Deleted: average

595

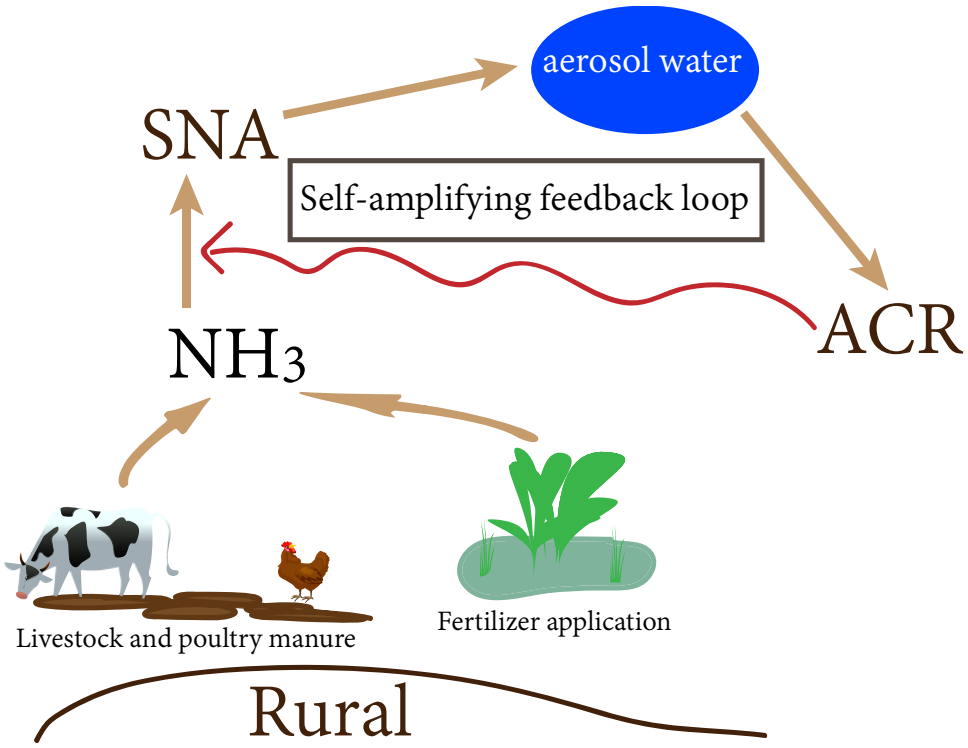

Figure 9: Schematic of self-amplifying feedback loop for SNA formation.

Deleted: 8

600

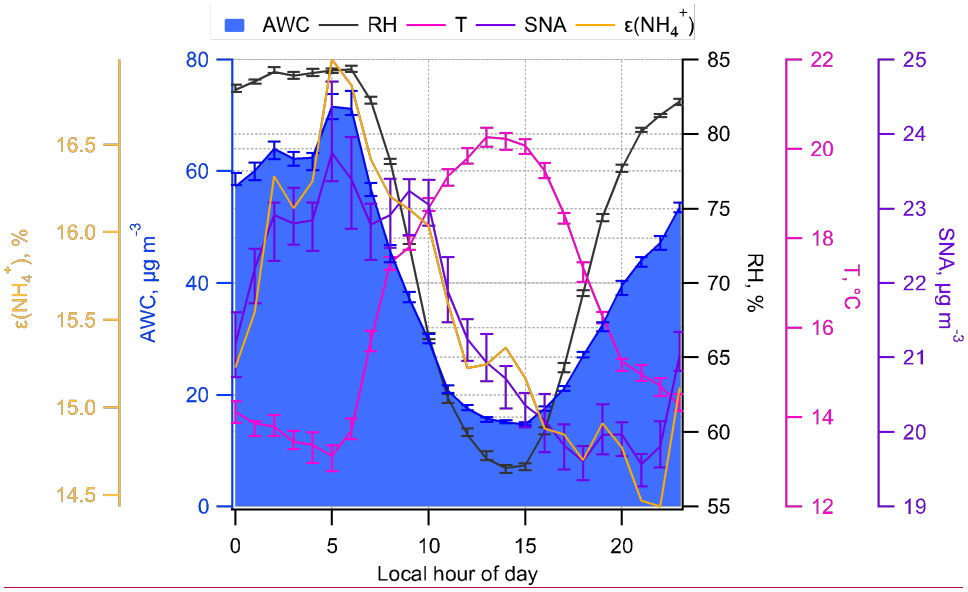

Figure 10: Annual mean diurnal pattern of $\varepsilon(NH_4^+)$, AWC, SNA, T, and RH.

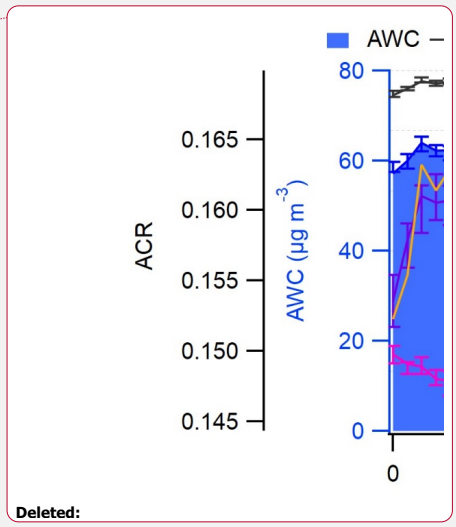

Deleted:

Deleted: 9

Deleted: ACR

Table 1. Statistical summary on mass concentrations of $PM_{2.5}$ species and NH_3.

Unit: μg m^{-3}	$PM_{2.5}$	SO_4^{2-}	NO_3^-	Cl^-	NH_4^+	NH_3
non-haze	28.5 ± 16.9	5.6 ± 3.6	6.9 ± 6.6	1.1 ± 0.9	5.6 ± 3.3	32.2 ± 11.6
haze	98.3 ± 37.2	13.3 ± 7.7	23.1 ± 14.5	2.2 ± 1.9	13.2 ± 6.6	32.3 ± 13.5

Table 2: The summer and winter mean (±1σ) $\varepsilon(NH_4^+)$, pH, T, activity coefficients ratio of $\frac{\gamma_{H^+}}{\gamma_{NH_4^+}}$, and NH_3 (μg m^{-3}) during the haze period.

	$\varepsilon(NH_4^+)$	AWC	pH	NH_3	$\frac{\gamma_{H^+}}{\gamma_{NH_4^+}}$	T
summer	0.2 ± 0.1	79 ± 73	3.4 ± 0.5	40 ± 8	1.9 ± 0.9	29 ± 5
winter	0.4 ± 0.1	115 ± 131	4.6 ± 0.3	20 ± 4	4.0 ± 4.7	5 ± 4

Deleted: ¶
Deleted: 1
Deleted: average
Deleted: ACR
Deleted: 8
Deleted: 1.7
Deleted: 2.7
Deleted: 2.2